

UNCLASSIFIED

AD 261 961

*Reproduced
by the*

ARMED SERVICES TECHNICAL INFORMATION AGENCY
ARLINGTON HALL STATION
ARLINGTON 12, VIRGINIA



UNCLASSIFIED

NOTICE: When government or other drawings, specifications or other data are used for any purpose other than in connection with a definitely related government procurement operation, the U. S. Government thereby incurs no responsibility, nor any obligation whatsoever; and the fact that the Government may have formulated, furnished, or in any way supplied the said drawings, specifications, or other data is not to be regarded by implication or otherwise as in any manner licensing the holder or any other person or corporation, or conveying any rights or permission to manufacture, use or sell any patented invention that may in any way be related thereto.

CATALOGED BY ASTIA
AS AD No. 261961

NOX

U.S. ARMY
H-25 HELICOPTER DROP TEST
22 October 1960

By
James W. Turnbow, Ph.D.

AvCIR

TREC
Technical Report 60-76

AvCIR 2-TR-125

March 1961

AVIATION CRASH INJURY RESEARCH

A DIVISION OF
FLIGHT SAFETY FOUNDATION, Inc.
PHOENIX, ARIZONA

**BLANK PAGES
IN THIS
DOCUMENT
WERE NOT
FILMED**

TCREC-ADR 9R95-20-001-01

SUBJECT: U. S. Army H-25 Helicopter Drop Test Report

TO: See Distribution List

1. The inclosed TREC Technical Report 60-76, "U. S. Army Helicopter Drop Test, 22 October 1960," was prepared by Dr. James W. Turnbow, Consulting Project Engineer to Aviation Crash Injury Research (AvCIR), a division of Flight Safety Foundation, Inc., under the provisions of Contract DA 44-177-TC-624. Conclusions derived from data presented in the report are concurred in by this Command.


2. Contents of this report represent a refinement of information contained in TREC Technical Report 60-75, "H-25 Helicopter Drop Test, Preliminary Report." In comparing the two reports, you will note differences with respect to the G Force measurements recorded at various stations. This is to be expected since the test was conducted without any filtering being introduced between the transducers and recorders, and it was necessary to smooth the accelerometer data as previously anticipated.

3. Dynamic crash test experimental research has been accelerated this year. Four additional crash tests have been conducted, and the program for 1962 will include full-scale drone operations, with particular emphasis being placed on the problem of crash and post-crash fires. Results of all experiments will be correlated to form a basis for recommending changes to existing military specifications, developing improved aircraft design criteria, and, in general, increasing to the maximum extent possible the chance of personnel survival in survivable-type aircraft accidents.

4. We would appreciate receiving your comments, if any, relative to this report. Correspondence should be addressed to: Commanding Officer, U. S. Army Transportation Research Command, Fort Eustis, Virginia, marked for the attention of the Research Analysis Division, Aviation Directorate.

FOR THE COMMANDER:

1 Inc.
a/s


RAPHAEL F. GAROFALO
CWO-4, USA
Assistant Adjutant

TREC Technical Report 60-76
AvCIR 2-TR-125

U. S. ARMY
H-25 HELICOPTER
DROP TEST

22 October 1960

TECHNICAL REPORT

prepared under

U. S. ARMY
TRANSPORTATION RESEARCH COMMAND
Contract DA-44-177-TC-624

By
James W. Turnbow, Ph. D.
Consulting Project Engineer
Professor of Engineering Science
Arizona State University

AVIATION CRASH INJURY RESEARCH
A Division of
Flight Safety Foundation, Inc.

15 March 1961

BLANK PAGE

TABLE OF CONTENTS

	<u>Page</u>
LIST OF TABLES AND ILLUSTRATIONS	v
SUMMARY	1
INTRODUCTION	3
TEST OBJECTIVES	5
TEST CONDITIONS	7
TEST SETUP	9
Test Method	9
Lift System	10
Automatic Triggering Device	10
Identification Markings	11
Instrumentation	14
TEST PROCEDURE	29
Pre-crash Tests	29
Crash Test	29
TEST RESULTS	31
General	31
Oscillograph Data	36
OCCUPANT INJURIES	65
Pilot	65
Passenger	65
Fire	66

TABLE OF CONTENTS (cont'd.)

	<u>Page</u>
CONCLUSIONS	69
APPENDIX A - Various Methods of Simulating Crash Conditions . .	71
APPENDIX B - Development-Testing of Energy Absorption System for the Shock-Mounting of Airborne Electronic Equipment	81
APPENDIX C - Data Reduction and Interpretation	91
APPENDIX D - Accelerometer Data Sign Convention	97

LIST OF TABLES AND ILLUSTRATIONS

Table		Page
1	Transducer Locations	16
 Figure		
1	Actual Test Conditions	6
2	Test Specimen Ready for Check Drop	8
3	Internal View Before Crash	8
4	Helicopter Ready for Crash Run	9
5	View Showing Lift System.	10
6	Automatic Triggering Device	11
7	Front View Showing Identification Markings	12
8	Layout at Test Site	13
9	Stadia Poles at Drop Site	14
10	Instrumentation Data Sensor Installations	19
11	Recording Equipment Installation	21
12	Airborne Instrumentation Package	22
13	View Showing External Cameras	22
14	View of Internal Side Camera	23
15	Interior View Showing (1) Airborne Instrumentation Package, (2) Shock Device, and (3) Aft Camera	23
16	Instrumentation Equipment on Crane	25
17	Umbilical Cable Pay-Off System	25
18	FSF Oscillograph Shock-Mount Showing Energy Absorption Device After Test Drop	27

LIST OF TABLES AND ILLUSTRATIONS (cont'd.)

Figure		Page
19	Dummy- Load Installation	30
20	Post-Crash Front View	33
21	Post-Crash Front Quarter View	33
22	Post-Crash View of Right Main Landing Gear	34
23	Post-Crash View of Dummy Pilot	34
24	Post-Crash View of Dummy Passenger	35
25	Post-Crash View of Cockpit	35
26	Acceleration and Velocity of Passenger Cabin Floor	44
27	Acceleration and Velocity of Cockpit Floor	45
28	Acceleration and Velocity of Passenger Chest	46
29	Acceleration, Velocity, and Displacement of Cockpit Floor	47
30	Comparison of Ground and Airborne Recording	48
31	Accelerations of Airborne Instrument Package	49
32	Cockpit Floor Accelerations	50
33	Passenger Cabin Floor Acceleration	51
34	Pilot Shoulder Harness and Seat Belt Loads and Pelvic Accelerations	52
35	Pilot Chest Accelerations	53
36	Passenger Seat Belt Loads and Chest Accelerations	54
37	Passenger Head Accelerations	55
38	Range Extender Tank Loads	56
39	Comparison of Horizontal and Vertical Accelerations for a C-46 Transport and an H-25A Helicopter	57

LIST OF TABLES AND ILLUSTRATIONS (cont'd.)

Figure		Page
40-1	Sequence Photograph - H-25 Drop Test	58
40-2	Sequence Photograph - H-25 Drop Test	58
40-3	Sequence Photograph - H-25 Drop Test	59
40-4	Sequence Photograph - H-25 Drop Test	59
40-5	Sequence Photograph - H-25 Drop Test	60
40-6	Sequence Photograph - H-25 Drop Test	60
40-7	Sequence Photograph - H-25 Drop Test	61
40-8	Sequence Photograph - H-25 Drop Test	61
41	Pilot Dummy Position Before and After Impact	62
42	Position of Pilot's Feet Before and After Impact . . .	63
43	Range Extender Tank Failures	64
44	Passenger Dummy Arm Failure	67
A-1	Proposed Test Method of Dropping Specimen onto 50° Inclined Plane	75
A-2	Proposed Layout for Swinging Helicopter As a Pendulum .	77
A-3	Proposed Layout for Test Using Monorail System	78
A-4	Proposed Test Method of Using Moving Crane to Drop Helicopter on Target While Moving at 35 Miles Per Hour .	80
B-1	Oscillograph Shock-Mount Test Set-Up Showing Energy Absorption Device and Electronic Package Before Drop	85
B-2	Set-Up for Test of Oscillograph Shock-Mount	87
B-3	Oscillograph Shock-Mount Test Ready for a Drop	88
B-4	Oscillograph Shock-Mount Test Post-Drop View	88
D-1	Accelerometer Data Sign Convention	99

SUMMARY

No technical crash-performance data presently exists for rotary wing and VTOL aircraft, i. e., data obtained under conditions permitting engineering measurements to be made during the accident. As a consequence, our ability to design intelligently for crashworthiness does not match our ability to design for airworthiness. To reduce this deficiency in our technology, a long-range program, based on a series of progressive steps leading ultimately to full-scale droned crash tests, has been initiated by the Flight Safety Foundation in conjunction with the U. S. Army Transportation Research Command.

This report presents the results of an exploratory, experimental study. A Piasecki Model H-25A helicopter has been employed in recreating a typical accident approximating an unsuccessful attempt to attain autorotation from a low altitude power failure. Relatively high (50G to 100G) vertical and longitudinal accelerations have been observed for periods in the order of 10 milliseconds in an impact leaving the cabin area of the airframe reasonably intact. Failure of all seats occurred without failure of either seat belts or shoulder harness.

The instrumentation and research techniques used in (1) the measurement of the impact forces and accelerations, (2) the determination of the feasibility of the utilization of on-board recorders, and (3) the evaluation of certain problems inherent in the dynamic crash testing of full-scale helicopter and VTOL aircraft were presented in an earlier preliminary report.*

* Preliminary Report - U. S. Army H-25 Helicopter Drop Test,
22 October 1960, AvCIR-1-TR-124, TREC Technical Report 60-75.

BLANK PAGE

INTRODUCTION

Through Contract DA-44-177-TC-624 between the U. S. Army Transportation Research Command (TRECOM) and the Flight Safety Foundation (FSF), Aviation Crash Injury Research (AvCIR), a division of FSF, was given the responsibility for the accomplishment of certain tasks in an extensive program initiated by TRECOM for the promotion of Army Aviation Safety. Among these tasks were (1) the crash-testing of representative types of aircraft for the purposes of study of structural integrity, and (2) the experimental evaluation of safety devices, crew and passenger restraint systems, and auxiliary equipment. There is currently in the literature almost no engineering data pertaining to crashes of rotary wing aircraft. Thus, because of the interest and need of the Army for the exploitation of the capabilities of such aircraft, it was urgent that rapid progress in the experimental testing of this equipment be made.

In May 1960, a paper, "Preliminary Considerations for Dynamic Testing of Aircraft and Their Components", was submitted to TRECOM. This was followed during the first week of July 1960 by the issuance of a specification and request for bids covering the instrumentation of an H-25A Piasecki helicopter for a crash test. Seven proposals were received and evaluated, and a sub-contract was awarded to the Aeronautics Division of the Chance Vought Aircraft Corporation, Dallas, Texas, on 1 August 1960.

The test was conducted on 22 October 1960 through the joint efforts of Chance Vought and AvCIR.

The development of the drop-test system used in producing the crash, the preparation of the aircraft exclusive of instrumentation, and the evaluation of the data were accomplished by the AvCIR staff.

BLANK PAGE

TEST OBJECTIVES

The objectives of this test program as outlined in reference (1)* were as follows:

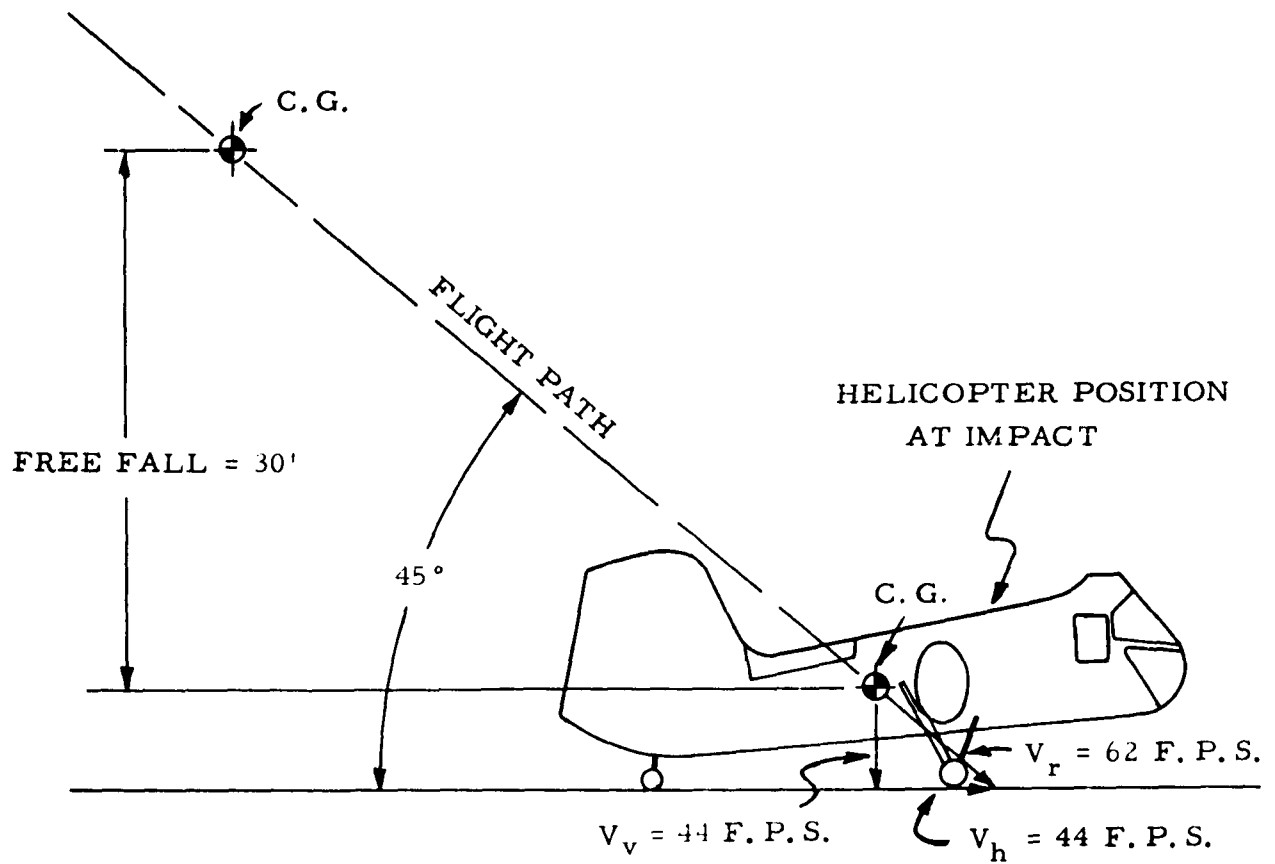
1. To measure crash forces on pilot and/or passenger seats, seat tie-down structure, floor structure, and other components of a rotary-wing aircraft affecting occupant protection in aircraft accidents.
2. To determine the feasibility of airborne recording and the reliability of photographic and electronic recording equipment.
3. To make general determinations of problems inherent in experimental dynamic testing for use in the design of subsequent experiments of a more complex nature.

The accomplishment of Objective No. 1 now provides information which may be used for more accurate interpretation of existing post-crash data obtained from studies of actual accidents.

Successful fulfillment of Objective No. 2 was considered an important step toward final instrumentation of drone aircraft requiring independent airborne recording systems.

Accomplishment of Objective No. 3 would prove valuable in the determination of test methods leading to the proper execution of future studies of a more complex nature.

* (1) Flight Safety Foundation Specification for Dynamic Testing by Vertical Drop Piasecki Helicopter Model No. H-25A, Serial No. ID 51-16637, dated 30 June 1960.



AVERAGE CRASH CONDITION:

FROM UNSUCCESSFUL AUTO-ROTATION
AFTER POWER FAILURE

FLIGHT PATH = 45° ANGLE WITH HORIZ.

FLIGHT PATH VELOCITY (RESULTANT VELOCITY)

$V_r = 41.7$ M. P. H. (61 F. P. S.)

VERTICAL VELOCITY $V_v = 30$ M. P. H. (44 F. P. S.)

HORIZONTAL (FORWARD) VELOCITY

$V_h = 30$ M. P. H. (44 F. P. S.)

ATTITUDE = 9° NOSE UP WITH 6° ROLL LEFT, 5° YAW LEFT

Figure 1. Actual Test Conditions

TEST CONDITIONS

The conditions at impact, desired to simulate a typical accident configuration as determined by a study of known accidents, were as follows:

1. A rate of descent of 2,500 feet per minute or 29 miles per hour.
2. Angle of impact with the ground of 40 degrees.
3. Pitch angle with the ground: from 20° nose up to 20° nose down.
4. The conditions actually attained in this test are shown in Figure 1.

Two Alderson anthropomorphic dummies were placed inside the helicopter, one in the left-hand pilot's seat and the other in the forward side troop-seat of the passenger cabin. These dummies were instrumented to measure acceleration in various parts of the body. A Mark XII range extender fuel tank, filled with 200 pounds of colored water to simulate its normal fuel load, was placed in the right-hand copilot's seat. The main fuel cell contained 250 pounds of colored water. Sand ballast was added to bring the weight of the helicopter to 6,250 pounds, and the center of gravity location to the proper point. The forward and aft rotor blades were removed for the test.

A photograph of the test article is presented in Figure 2. A photograph of the interior of the test article is shown in Figure 3.

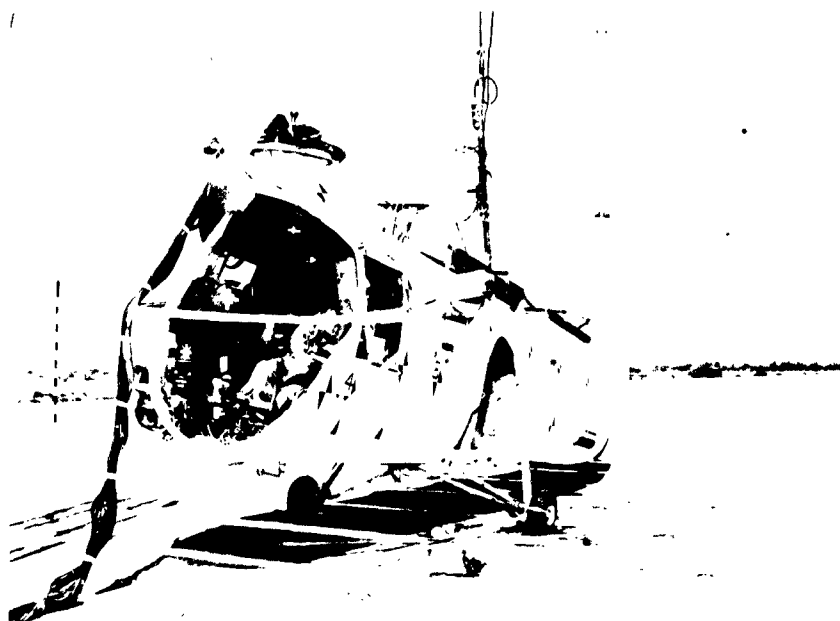


Figure 2. Test Specimen Ready for Check Drop



Figure 3. Internal View Before Crash

TEST SET-UP

TEST METHOD

Of four methods considered for establishing the impact conditions outlined under "TEST CONDITIONS", the method selected for the test consisted of dropping the helicopter from a moving crane.* The crane suspended the helicopter at the 30-foot free-fall height necessary to duplicate the required vertical velocity, with the forward velocity of the crane vehicle providing the forward velocity of the aircraft.

The suspended helicopter was stabilized in the pitch, yaw, and roll during the crane run by means of special fittings and cables on the crane boom.

A photograph showing the helicopter suspended from the crane as it was in the test run is presented in Figure 4.

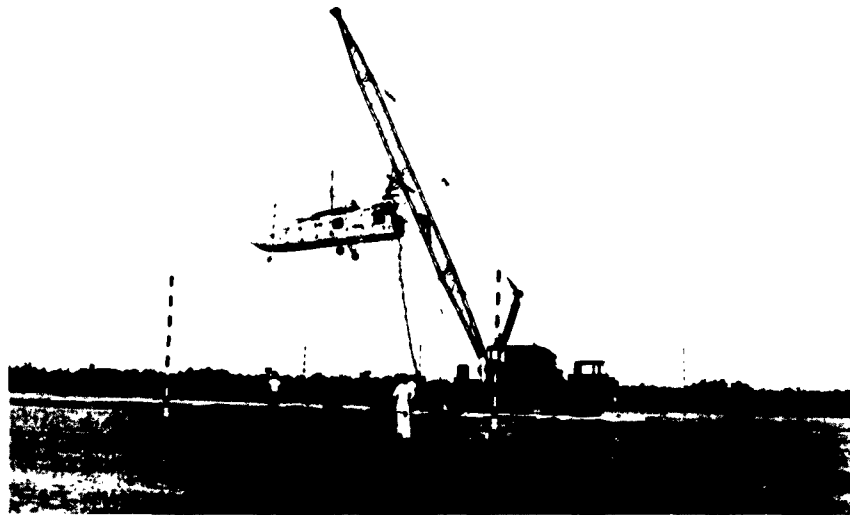


Figure 4. Helicopter Ready for Crash Run

* See Appendix A.

LIFT SYSTEM

A simple hoisting arrangement was used to lift the helicopter and suspend it during the crane run. Thin steel straps were attached to each side of the fuselage at five (5) points, and were connected to a channel framework to which the release hook was attached. A photograph showing the lift system installed on the helicopter is presented in Figure 5.

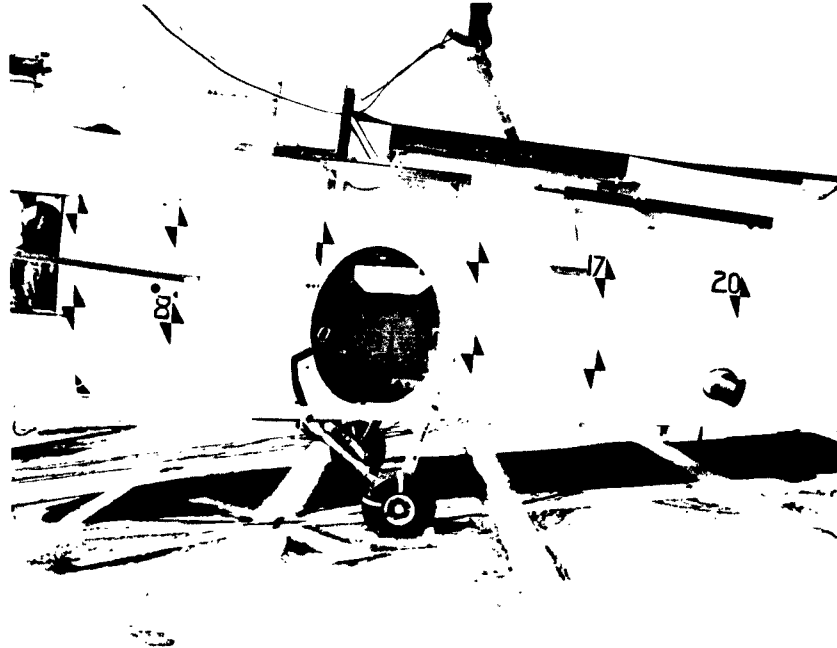


Figure 5. View Showing Lift System

AUTOMATIC TRIGGERING DEVICE

To release the helicopter and assure its impact on the target area, an automatic triggering device was employed using a spring-loaded switch held in place by a lever-arm. The switch was opened, and the helicopter was released when the lever-arm (mounted externally on the crane) was contacted by a stationary pole set on the ground at a predetermined distance from the impact point. The triggering device is shown in the photograph in Figure 6.

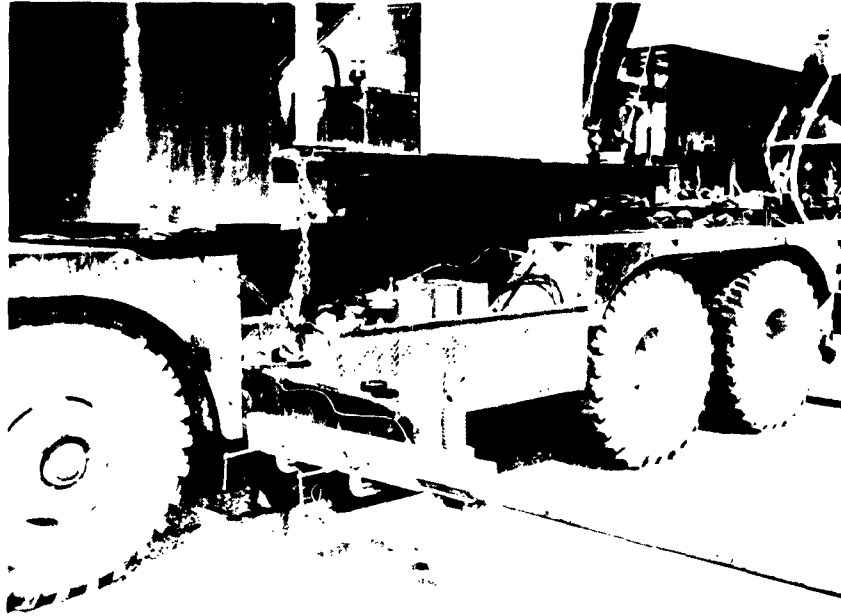


Figure 6. Automatic Triggering Device

IDENTIFICATION MARKINGS

To serve as an aid to the high-speed movie coverage, both the interior and exterior surfaces of the helicopter were painted white. Identification markings were placed on important helicopter structure such as landing gears, fuselage frames, seat supports, etc. using red reflective tape. Markings were placed on the exterior fuselage with black paint to assist in the determination of structural deformation. The fuel cell water in both the range extender fuel tank and the main fuel cell contained red dye to show the extent of fuel flow in case of cell rupture. Photographs showing identification markings are presented in Figures 3 and 7.

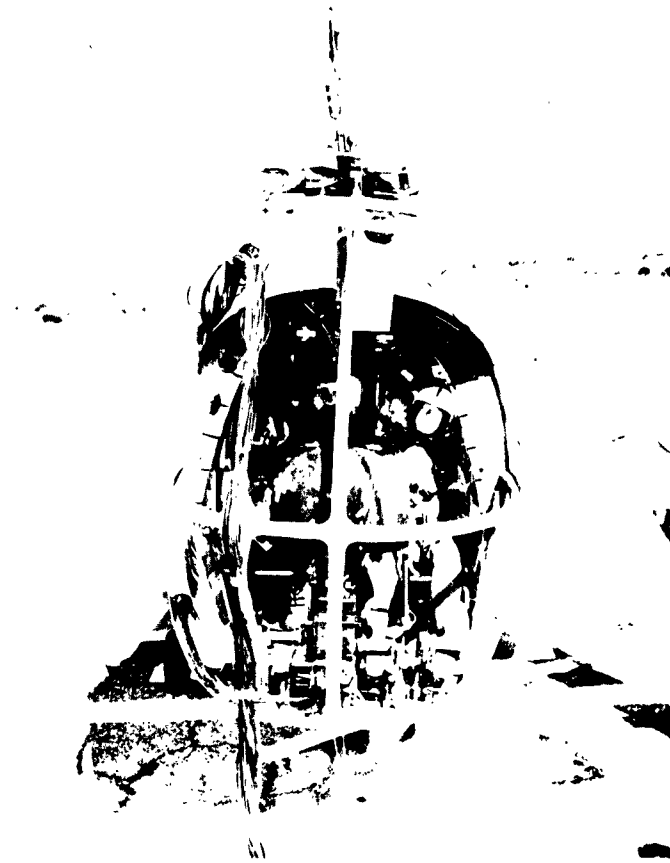
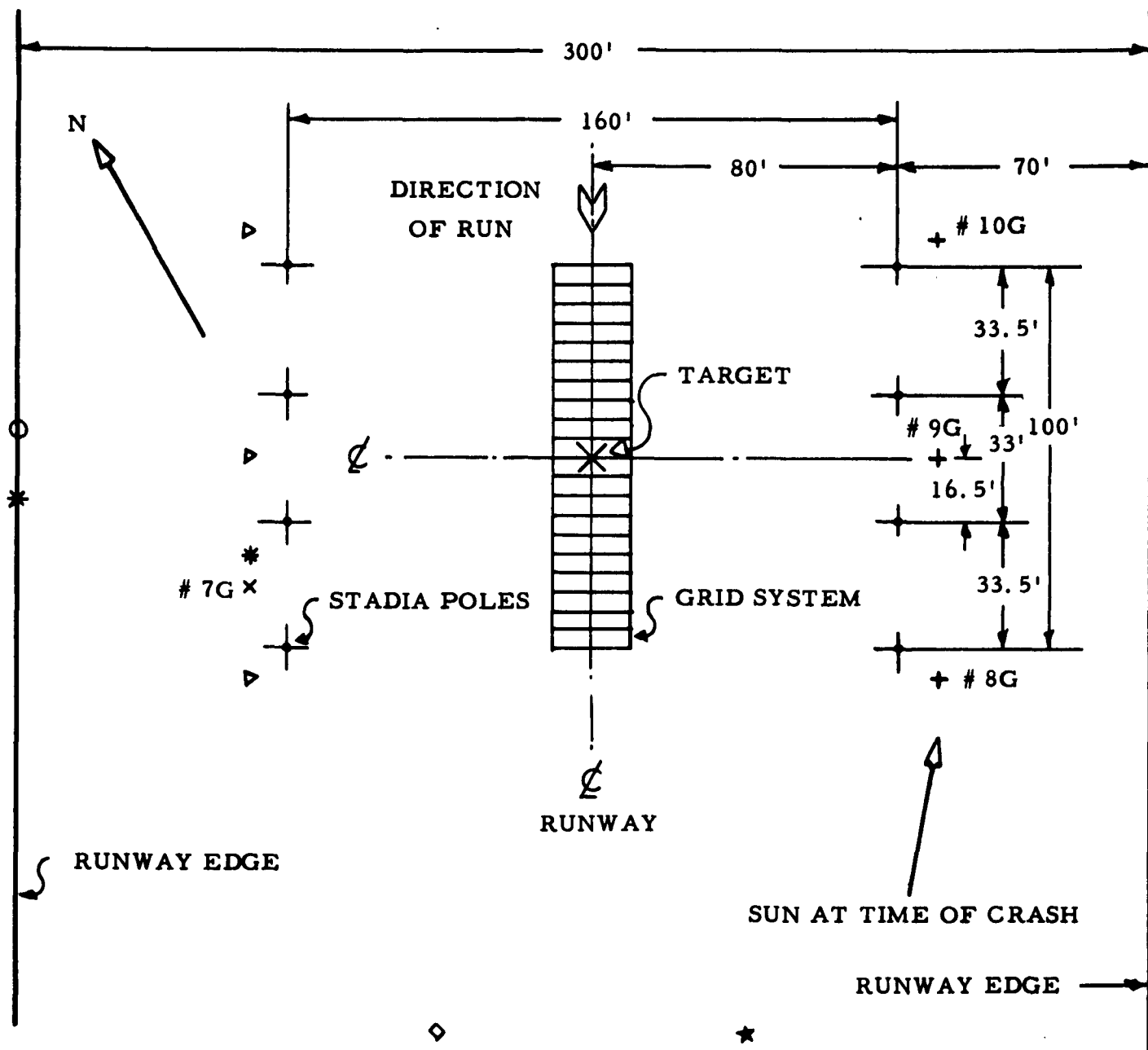


Figure 7. Front View Showing Identification Markings

A grid system, painted on the ground at the impact site, and eight 16-foot vertical stadia poles served as a reference system for the high-speed movie coverage. A sketch showing the layout at the crash site is presented as Figure 8.



Scale: 1" = 40'0"

SYMBOLS

- STADIA POLES - 8 TOTAL
- + CVA 16 MM. 1000 F.P.S. - 3 TOTAL (NOS. 8G, 9G, & 10G)
- x CVA 16 MM. 200 F.P.S. - 1 TOTAL (NO. 7G)
- * CVA 16 MM. 24 F.P.S. (DOCUMENTARY) - 2 TOTAL
- △ PHOTOSONICS 16 MM. HI-SPEED - 3 TOTAL
- PHOTOSONICS 35 MM. HI-SPEED - 1 TOTAL
- ★ U.C.L.A. 70 MM. 48 F.P.S. - 1 TOTAL
- FSF 16 MM. 32 F.P.S. - 1 TOTAL

Figure 8. Layout at Test Site

A photograph showing the test site, with stadia poles in place, is presented in Figure 9.

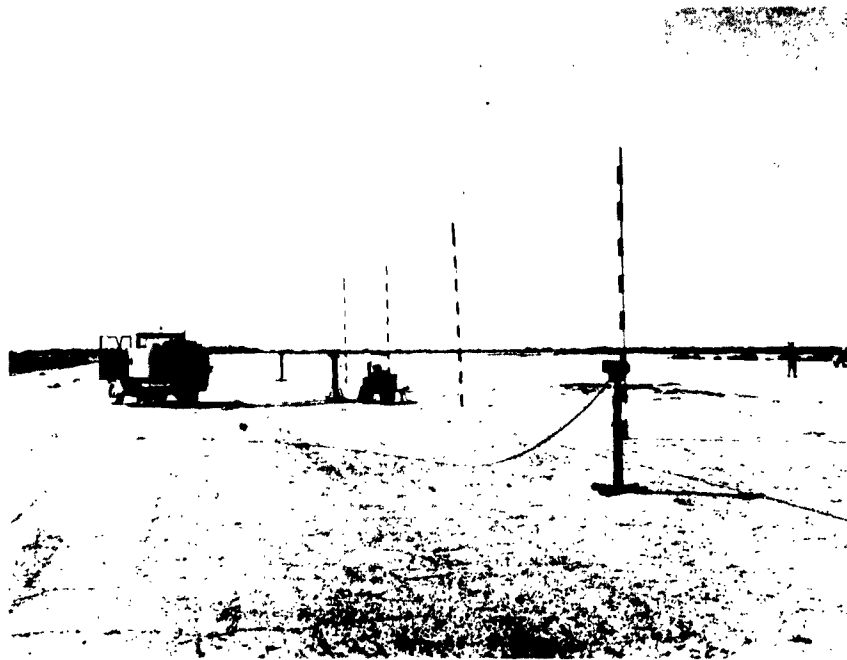


Figure 9. Stadia Poles at Drop Site

INSTRUMENTATION

Instrumentation of the test vehicle consisted of installing electronic pickups and cameras at the required locations and recording the data on independent airborne and ground recording systems. An umbilical cable was installed between the instrumentation pickups in the helicopter and the ground recording system.

Instrumentation Pickups

Strain gage type accelerometers were installed to measure vertical, longitudinal and/or lateral forces at the following points:

1. Cockpit floor
2. Passenger cabin floor
3. Pilot's seat
4. Chest cavity of anthropomorphic pilot dummy
5. Cranial cavity of anthropomorphic pilot dummy
6. Pelvis of anthropomorphic pilot dummy (vertical and longitudinal only)
7. Chest cavity of anthropomorphic passenger dummy
8. Cranial cavity of anthropomorphic passenger dummy
9. Fuel cell aft of firewall (vertical only)
10. Airborne oscillograph

A fuel cell pressure measurement was made using a strain gage type pressure transducer immersed in the main fuel cell cavity.

Strain gage type tensiometers were used to measure loads at the following points:

1. Shoulder harness of pilot dummy
2. Seat belt of pilot dummy (left and right tie points)
3. Shoulder harness of range extension fuel tank
4. Seat belts of range extension fuel tank (left tie point only)
5. Seat belt of passenger dummy (right tie point only)

Output signals from the above-listed instrumentation were recorded on two 18-channel ground and one 26-channel airborne oscillographs. Eight of the channels were simultaneously recorded on both the ground and airborne recorders. A complete listing of instrumentation to each oscillograph is presented in Table 1. A sketch showing sensor installations in the helicopter is presented in Figure 10.

TABLE I
TRANSDUCER LOCATIONS

Oscillo- graph No.	Channel	Instrumentation		MEASUREMENT	Force Direction	Fig. No.	Page No.
		Pick-up Type	Range				
	1	Accelerometer	50 G	Passenger Dummy-Chest Cavity	Lateral	36	54
	2	Accelerometer	10 G	Passenger Dummy-Chest Cavity	Longitudinal	36	54
	3	Impact Switch	BLIP	CORRELATION	-----	--	--
	4	Accelerometer	50 G	Passenger Dummy-Chest Cavity	Vertical	28,36	46,54
	5	Accelerometer	20 G	Passenger Cabin Floor	Lateral	33	51
	6	Accelerometer	100 G	Passenger Cabin Floor	Longitudinal	33	51
	7	-----	-----	-----	-----	--	--
1	8	Accelerometer	100 G	Passenger Cabin Floor	Vertical	26,33	44,51
	9	-----	-----	-----	-----	--	--
(Ground	10	Accelerometer	50 G	Passenger Dummy-Cranial Cavity	Lateral	37	55
System)	11	Accelerometer	100 G	Cockpit Floor	Vertical	27,32	45,50
	12	-----	-----	-----	-----	--	--
	13	Accelerometer	20 G	Cockpit Floor	Lateral	32	50
	14	Accelerometer	100 G	Cockpit Floor	Longitudinal	29,32	47,50
	15	Accelerometer	10 G	Passenger Dummy-Cranial Cavity	Longitudinal	37	55
	16	Accelerometer	50 G	Passenger Dummy-Cranial Cavity	Vertical	37	55
	17	Tensiometer	0 -				
			5000#	Passenger Dummy-Seat Belt	Tension	36	54
	18	A. C. Generator	60 cps	Timing	--	--	--

TABLE I, Cont'd.

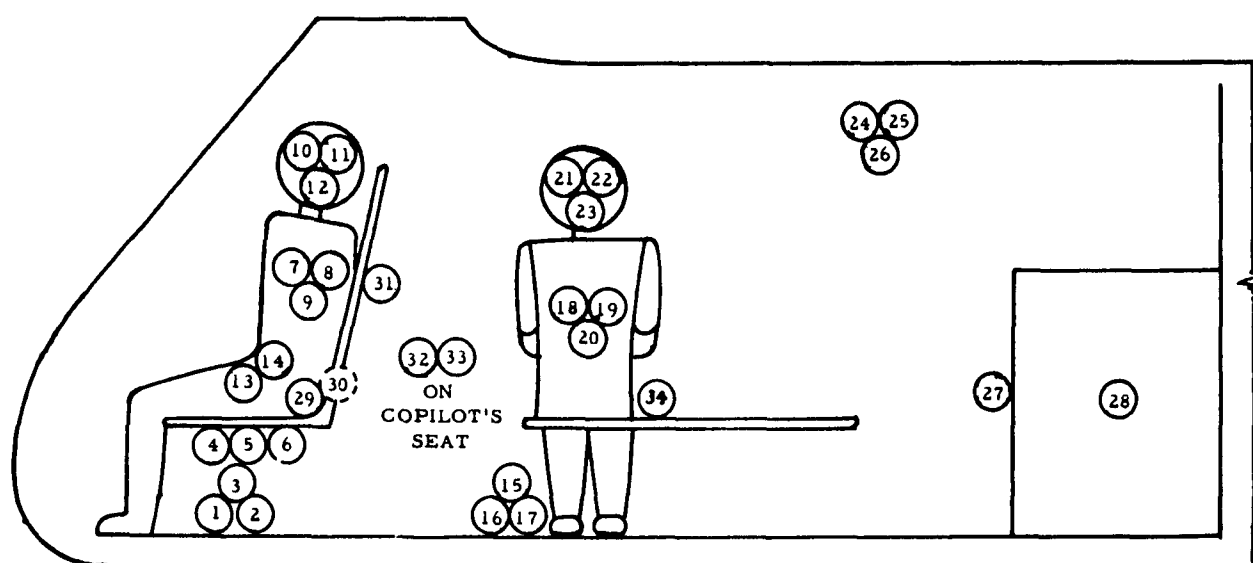
Oscillo- graph No.	Channel	Instrumentation		MEASUREMENT	Force Direction	Fig. No.	Page No.
		Type	Pick-up Range				
1		Accelerometer	10 G	Pilot Dummy-Chest Cavity	Lateral	35	53
2		Accelerometer	50 G	Pilot Dummy-Chest Cavity	Longitudinal	35	53
3		Impact Switch	BLIP	CORRELATION	-----	--	--
4		Accelerometer	50 G	Pilot Dummy-Chest Cavity	Vertical	35	53
5		-----	----	-----	-----	--	--
6		Accelerometer	50 G	Pilot Dummy-Pelvis	Longitudinal	34	52
7		Accelerometer	50 G	Pilot Dummy-Pelvis	Vertical	34	52
8		Tensiometer	0				
9	2 (Ground System)	Accelerometer	5000#	Pilot Dummy-Seat Belt LH.	-----	--	--
10		Accelerometer	10 G	Airborne Oscillograph	Lateral	31	49
11		Accelerometer	20 G	Airborne Oscillograph	Longitudinal	31	49
12		-----	----	-----	-----	--	--
13		Accelerometer	20	Airborne Oscillograph	Vertical	31	49
14		-----	----	-----	-----	--	--
15		Tensiometer	0 -				
16		-----	----	Pilot Dummy-Seat Belt RH.	Tension	34	52
17		Tensiometer	0 -	-----	-----	--	--
18		-----	----	Pilot Dummy-Shoulder Harness	Tension	34	52
		A. C. Generator	60 cps	Timing	-----	--	--

TABLE I Cont'd.

Oscillo- graph No.	Channel	Instrumentation		Range	MEASUREMENT		Force Direction	Fig. No.	Page No.
		Type	Pick-up						
	1	Accelerometer		± 10 G	Passenger Dummy-Chest Cavity		Lateral		*
	2	-----	-----	-----	-----	-----	-----	-----	-----
	3	Accelerometer		± 50 G	Passenger Dummy-Chest Cavity		Longitudinal		*
	4	Accelerometer		± 50 G	Passenger Dummy-Chest Cavity		Vertical	30	48
	5	-----	-----	-----	-----	-----	-----	-----	-----
	6	Accelerometer		± 20 G	Passenger Cabin Floor		Lateral		*
	7	Accelerometer		± 100 G	Passenger Cabin Floor		Longitudinal		*
	8	-----	-----	-----	-----	-----	-----	-----	-----
	9	Accelerometer		± 100 G	Passenger Cabin Floor		Vertical	30	48
	10	Accelerometer		± 50 G	Dummy Passenger-Cranial Cavity		Lateral		*
	11	-----	-----	-----	-----	-----	-----	-----	-----
	12	Accelerometer		± 100 G	Cockpit Floor		Vertical		*
	13	-----	-----	-----	-----	-----	-----	-----	-----
	14	Accelerometer		10 G	Pilot's Seat		Lateral		**
	15	Accelerometer		100 G	Pilot's Seat		Longitudinal		**
	16	Transducer		0-100 PSI	Fuel Cell Pressure		-----	-----	-----
	17	Accelerometer		± 100 G	Pilot's Seat		Vertical		**
	18	Accelerometer		± 10 G	Pilot Dummy-Cranial Cavity		Lateral		**
	19	Accelerometer		± 50 G	Pilot Dummy-Cranial Cavity		Longitudinal		**
	20	Accelerometer		± 100 G	Fuel Cell Wall-Sta. 173.6		Vertical		**
	21	Accelerometer		± 50 G	Pilot Dummy-Cranial Cavity		Vertical		**
	22	Tensiometer		0 - 5000#	Range Extension Fuel Cell - Seat Belt		Tension	38	56
	23	Tensiometer		0 - 5000#	Range Extension Fuel Cell - Shoulder Harness		Tension	38	56
	24	A. C. Generator		60 cps	Timing		-----	-----	-----
	25	Impact Switch		BLIP	CORRELATION		-----	-----	-----
	26	-----	-----	-----	-----	-----	-----	-----	-----

* See Oscillograph No. 1.

** Not presented in this report.



- | | |
|--|---|
| 1. Cockpit Floor Acceleration - Lateral | 16. Passenger Cabin Floor Acceleration - Longitudinal |
| 2. Cockpit Floor Acceleration - Longitudinal | 17. Passenger Cabin Floor Acceleration - Vertical |
| 3. Cockpit Floor Acceleration - Vertical | 18. Passenger Chest Acceleration |
| 4.* Pilot's Seat Acceleration - Lateral | 19. Passenger Chest Acceleration - Longitudinal |
| 5.* Pilot's Seat Acceleration - Longitudinal | 20. Passenger Chest Acceleration - Vertical |
| 6.* Pilot's Seat Acceleration - Vertical | 21. Passenger Head Acceleration - Lateral |
| 7. Pilot's Chest Acceleration - Lateral | 22. Passenger Head Acceleration - Longitudinal |
| 8. Pilot's Chest Acceleration - Longitudinal | 23. Passenger Head Acceleration - Vertical |
| 9. Pilot's Chest Acceleration - Vertical | 24. Equipment Package Acceleration - Lateral |
| 10.* Pilot's Head Acceleration - Lateral | 25. Equipment Package Acceleration - Longitudinal |
| 11.* Pilot's Head Acceleration - Longitudinal | 26. Equipment Package Acceleration - Vertical |
| 12.* Pilot's Head Acceleration - Vertical | 27.* Fuel Tank Acceleration - Vertical |
| 13. Pilot's Pelvis Acceleration - Longitudinal | 28.* Fuel Tank Pressure |
| 14. Pilot's Pelvis Acceleration - Vertical | 29. Pilot's Seat Belt Force (Right) |
| 15. Passenger Cabin Floor Acceleration - Lateral | 30. Pilot's Seat Belt Force (Left) |
| | 31. Pilot's Shoulder Harness Force |
| | 32.* Fuel Tank Seat Belt Force |
| | 33.* Fuel Tank Shoulder Harness Force |
| | 34. Passenger Seat Belt Force |

* Recorded on airborne oscillograph only.

Figure 10. Instrumentation Data Sensor Installations

Recording Systems

1. Airborne System

The airborne oscillograph recording and photographic systems, having their own power sources, were independent of the ground system except that the ground calibrator was used for calibration of the airborne oscillograph. The airborne setup included the following equipment:

a. Oscillograph Recording System

- (1) 1 - CEC 5-122 Oscillograph (26-channel)
- (2) 1 - Leland SE-2 Inverter
- (3) 1 - CEC 5-053 Timer

b. Photographic Recording System

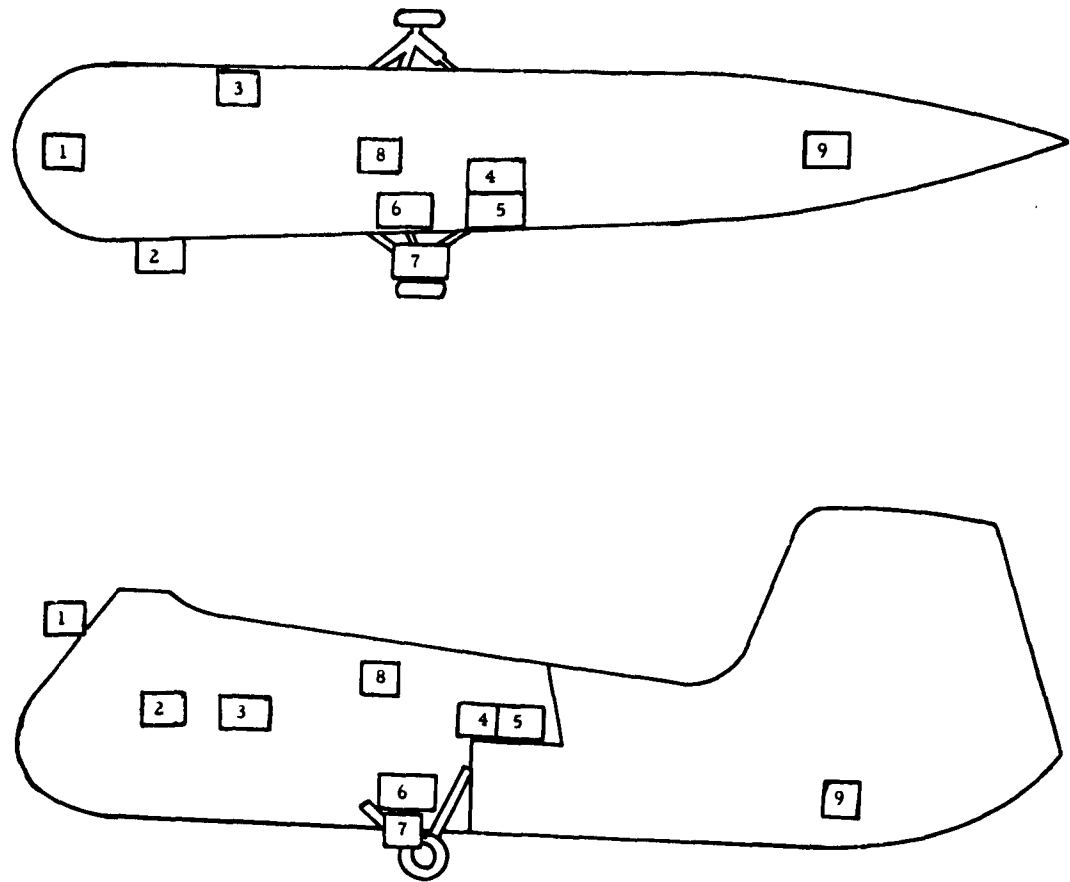
- (1) 2 - Photosonics Hi-Speed Camera with 5.3 mm. Wollensak lens
- (2) 1 - Photosonics Hi-Speed Camera with right angle optical system and 5.3 mm. Wollensak lens
- (3) 1 - Photosonics Hi-Speed Camera with 1/2-inch f2.3 Wollensak lens
- (4) 2 - Bell & Howell Gunsight Camera

c. Airborne Systems Power Supply

- (1) 3 - Sonotone 10H120 (30V) Nicad Battery

A sketch showing location of airborne equipment is presented in Figure 11. A detailed description of the airborne recording system, including circuit diagrams, was presented in the preliminary report. * Photographs showing the airborne instrumentation package and camera installations are presented in Figures 12 through 15.

* Preliminary Report - U. S. Army H-25 Helicopter Drop Test,
22 October 1960, AvCIR-1-TR-124, TREC Technical Report 60-75.



- | | |
|-----------------------------|---------------------------|
| 1. HIGH SPEED CAMERA NO. 1A | 8. EQUIPMENT PACKAGE |
| 2. HIGH SPEED CAMERA NO. 2A | CONTAINING: |
| 3. HIGH SPEED CAMERA NO. 3A | A. CEC 5-122 OSCILLOGRAPH |
| 4. HIGH SPEED CAMERA NO. 4A | B. CEC TIMER |
| 5. LOW SPEED CAMERA NO. 5A | C. LELAND INVERTER |
| 6. LOW SPEED CAMERA NO. 6A | D. RELAYS |
| 7. IMPACT SWITCH | 9. BATTERIES |

Figure 11. Recording Equipment Installation

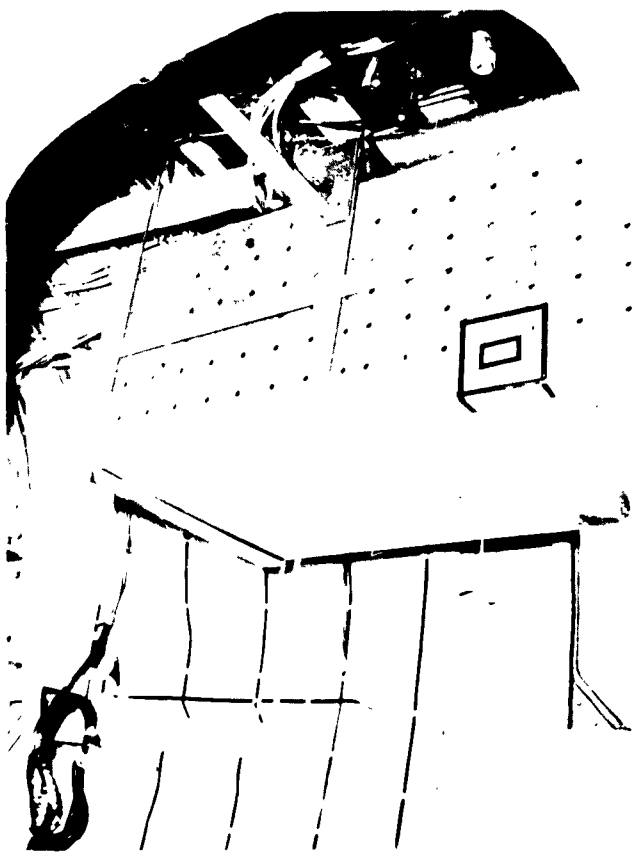


Figure 12. Airborne
Instrumentation Package

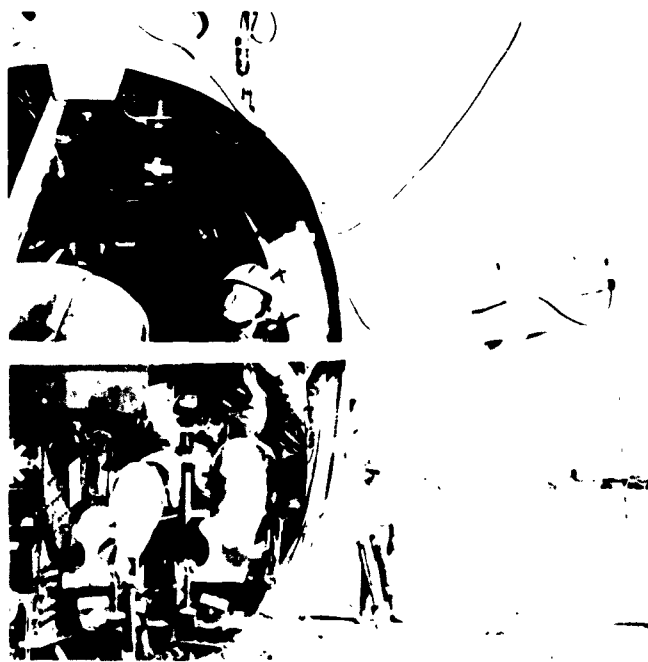


Figure 13. View Showing
External Cameras

Figure 14. View of Internal
Side Camera

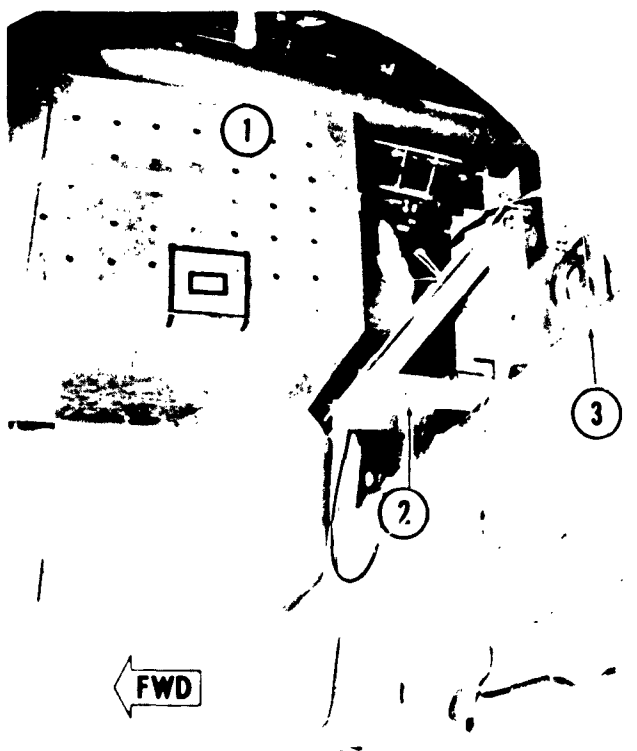
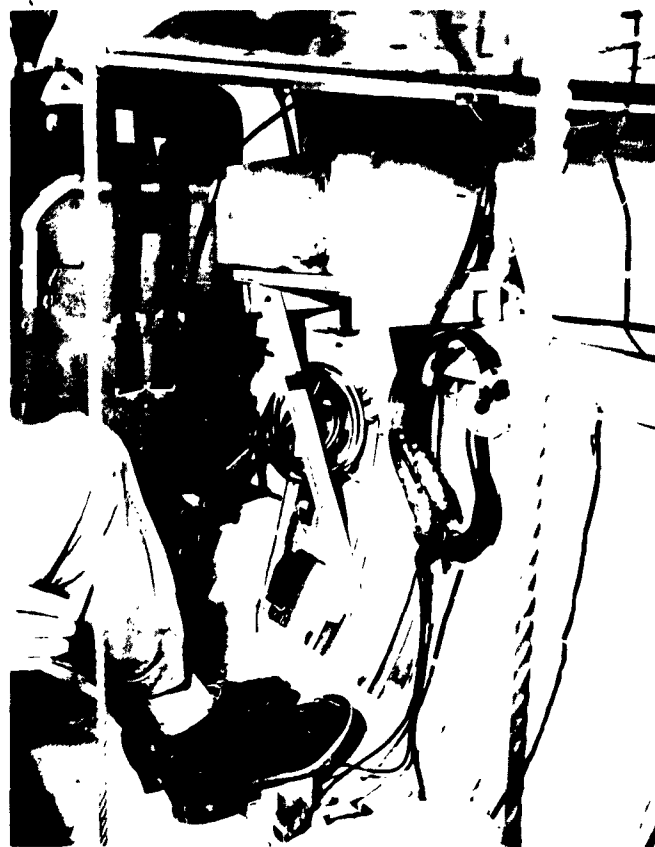


Figure 15. Interior View Show-
ing (1) Airborne Instrumentation
Package, (2) Shock Device,
and (3) Aft Camera

2. Ground System

The ground oscillograph recording system, having its own power supply, was shock-mounted to the rear deck of the drop crane. The ground photographic system and its power source was located on the ground near the crash site. The ground setup included the following equipment:

a. Oscillograph Recording System

- (1) 2 - CEC 5-114 Oscillograph (18-channel)
- (2) 1 - CVA Calibrator (36-channel)
- (3) 1 - Sonotone 20H120 (12V) Nicad Battery
- (4) 1 - 23V Lead Acid Battery
- (5) 1 - PE75 Auxiliary Power Unit (U. S. Army)
115V-AC, 2.5 KW

b. Photographic Recording System

- (1) 4 - Fairchild Hi-Speed Cameras
- (2) 1 - 110V AC Power Unit
- (3) 1 - 28V DC Power Unit

A detailed description of the ground recording system, including circuit diagrams, is presented in the preliminary report.* A photograph showing the ground instrumentation system mounted on the drop crane is presented as Figure 16.

Umbilical Cable

The umbilical cable installed between airborne instrumentation pickups and the ground recording system located on the crane deck had a maximum play-out length of 100 feet. A disconnect panel was provided should the distance between the helicopter and crane exceed this length. A photograph showing the cable in place on the drop crane is presented in Figure 17.

* Preliminary Report - U. S. Army H-25 Helicopter Drop Test,
22 October 1960, AvCIR-1-TR-124, TREC Technical Report 60-75.

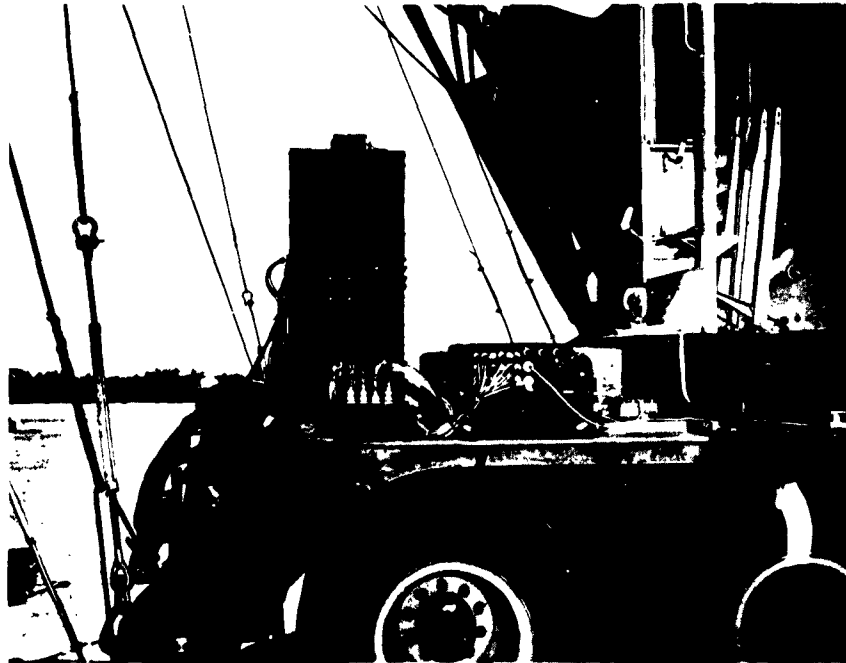


Figure 16. Instrumentation Equipment on Crane

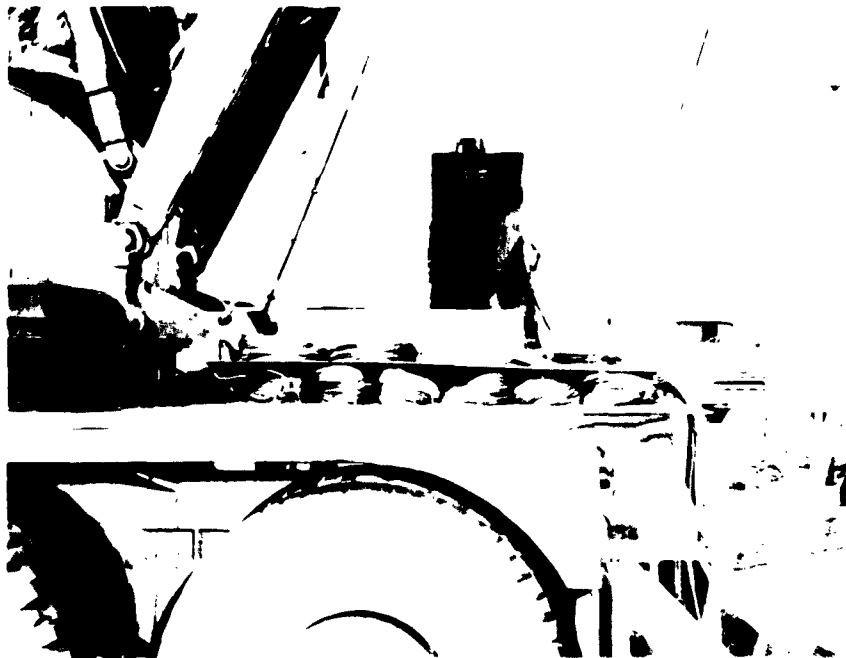


Figure 17. Umbilical Cable Pay-Off System

Instrumentation Details

1. End Instrument Artery Circuit

The end instruments, consisting of twenty-seven accelerometers and six force links, were connected to the calibrator installed on the crane deck by thirty-three Belden #8424 shielded cables. The outputs of the calibrator were connected through Belden #8422 shielded cable to the galvanometer inputs on each oscillograph.

2. Event Correlation Circuit

An impact switch mounted on the left landing gear was used to provide an event correlation signal to the three oscillographs and a firing voltage for three flashbulbs. One flashbulb was attached to the chest of the pilot in the field of view of cameras 1A and 2A. The second flashbulb was attached to the right side of the passenger dummy's head in the field of view of cameras 3A and 4A. The remaining flashbulb was attached to the forward rotor housing in the field of view of all the ground cameras. The signal from the switch simultaneously fired the flashbulbs and recorded a blip on all three oscillograph records.

3. Oscillograph and Airborne Camera Timing

A 60 cps signal from the 2.5 KW generator mounted on the drop crane was recorded simultaneously on each oscillograph record and on the film in all airborne high-speed cameras. This trace was used to correlate data between the oscillograph records and the film.

4. Oscillograph Calibration Circuit

Just prior to and immediately after the crash drop of the helicopter, an automatic resistance calibration was made for all channels of the oscillograph recording system. This calibration was accomplished by utilizing an automatic calibrator which applies known voltage of the same orders of magnitude as those obtained by straining the gages of the bridges.

Shock Mounting of Airborne Instrumentation Package

Since proper operation of the airborne oscillograph, timer, and inverter could not be guaranteed at accelerations exceeding 15 G's, it was necessary to shock-mount this equipment. The container designed to house this equipment included styrofoam packing up to 4 inches thick around the equipment to protect it in case of failure of the energy absorption system. Energy absorption devices, capable of reducing the "G" loading on the equipment to the acceptable 15 G limit, were designed using Dow styrofoam, density 2 pounds per cubic foot, as the energy absorption material. Since space within the helicopter was limited, a 5:1 pulley arrangement was used to reduce the size of the styrofoam block required.

Two separate energy absorption devices were installed in the helicopter for the crash tests. The vertical shock device limiting the maximum loading to the electronic package to 12.0 G's was mounted externally on top of the helicopter. The longitudinal shock device limiting the maximum loading to the electronic package to 8.0 G was mounted in the helicopter on the shelf above the main fuel cell. The resultant design loading on the electronic package from the simultaneous loading of the two devices was 14.5 G.

A photograph showing the energy absorption design, typical for both the vertical and longitudinal systems, is presented in Figure 18.

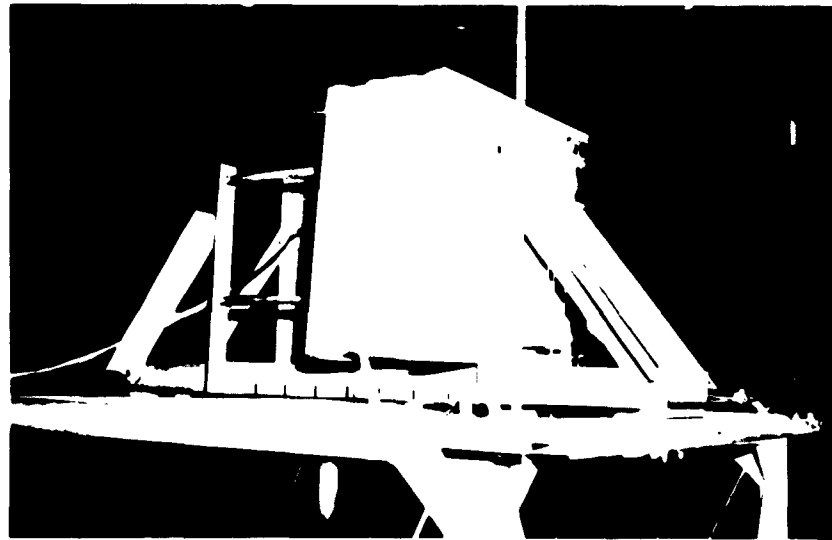


Figure 18. FSF Oscillograph Shock-Mount
Showing Energy Absorption Device
After Test Drop

A view showing the vertical device installed in the helicopter is presented in Figure 5. * A comprehensive presentation of the design, development, testing, installation of the shock devices and airborne oscillograph is given in Appendix B.

* For further details concerning the instrumentation, see Preliminary Report - U. S. Army H-25 Helicopter Drop Test, 22 October 1960, AvCIR-1-TR-124, TREC Technical Report 60-75.

TEST PROCEDURE

PRE-CRASH TESTS

Log Tests

Tests were made to determine the ability of the crane to transport the helicopter at the required speed and drop it in the desired target area. The tests were made using a 6,000-pound bundle of logs to simulate the mass of the helicopter. The following items were observed during the tests:

1. The acceleration and maximum speed of the crane;
2. Stability of the suspended mass during the run;
3. Function of the automatic triggering device and release hook;
4. Ability to drop the mass at the desired point;
5. Functioning of the umbilical cable pay-out system; and
6. Ability of the crane to decelerate the load in event of a failure of the release system.

Check Drop

Prior to the actual crash drop, two drops of the helicopter were made from a height of 6 inches to check the operation of the electronic equipment. Test shots were made with the on-board cameras during the first of these drops.

A photograph showing the logs in position for a test run is presented in Figure 19.

CRASH TEST

After the final pre-drop servicing of the landing gear tires and the shock-struts had been completed and the final instrumentation check-out had been made, the helicopter was hoisted into position on the crane boom. The runway in the immediate target area was swept free of dust a few minutes prior to the crash.

The crane run commenced some 4,000 feet from the impact point so that the crane would have sufficient running distance to reach the required speed of 30 MPH. Flags were placed on each side of the runway 100

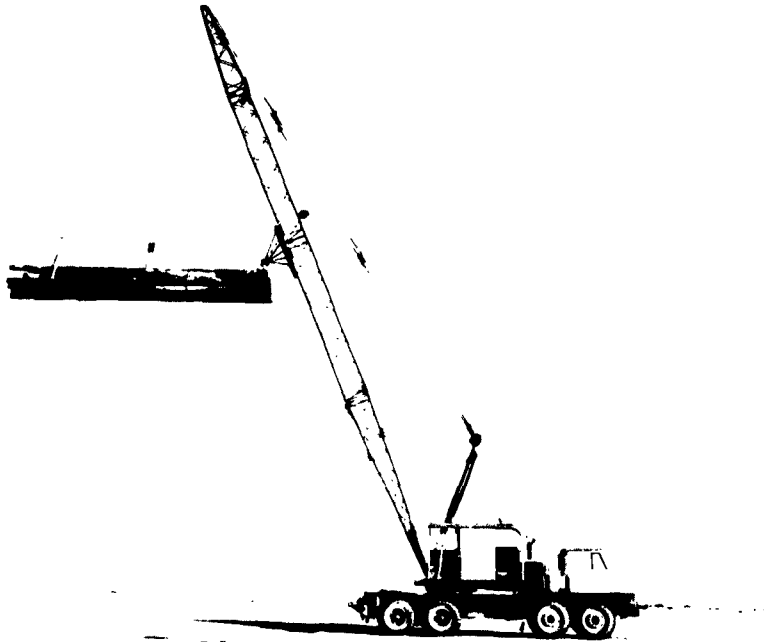


Figure 19. Dummy- Load Installation

feet prior to the release point to signal the operator to switch on the instrumentation equipment and energize the release-hook safety 2 seconds prior to the drop. The release hook was triggered at the instant of contact of the arm of the automatic triggering device with the stationary ground pole located 54 feet behind the impact point.

The fall and impact of the helicopter was recorded by high-speed movie cameras installed in the helicopter and on the ground.

A photograph showing the helicopter hoisted into position on the crane boom and ready for the crash run is presented in Figure 4.

TEST RESULTS

GENERAL

The drop was made at 1615 MST on 22 October 1960. The weather was fair except for a thin scattering of cirrus clouds which intermittently affected sunlight intensity. The temperature was approximately 80 degrees F. A cross-wind of approximately 5 knots was observed.

During the 4,000-foot run, the crane accelerated smoothly to a maximum speed of 30 miles per hour as in previous log test runs. The suspended helicopter was observed to be slightly swaying as it neared the target area. The center of the helicopter impacted at a point 2 feet to right and 3 feet forward of target dead center. During the free fall, the vehicle was observed to roll slightly to the left and yaw to the left; the roll angle measured approximately 6 degrees, the yaw angle approximately 5 degrees at ground contact. There was no pitching of the vehicle. The helicopter moved forward after ground contact a distance of 16 feet.

A post-crash examination was made to determine the extent of damage to the vehicle and injury to its occupants. The following observations were made:

1. Helicopter Structure

At ground contact, the light fuselage structure was pushed in by the stiffer landing gear, causing considerable distortion to the fuselage around the gear and internal buckling of the fuselage floor in the region of the forward landing gear attachments. The outer shell of the helicopter did not greatly distort except on the underside; however, there were a number of skin penetrations and breaks. (See Figures 20 through 25.) The occupant area, although distorted, was essentially intact.

2. Pilot

The pilot seat support-structure collapsed through buckling of the front legs and the dummy pilot's head struck the fuselage frame on the left hand side of the cockpit violently enough to split his helmet visor and crack the helmet; however, the helmet remained intact and was not permanently dented. (See Figure 23.) The right foot had been pushed under or around the right torque pedal.

3. Passenger

The troop seat collapsed in such a manner that the passenger dummy was thrown forward and downward, his head contacting the rear of the pilot's seat with no apparent damage to the helmet. The left arm of the dummy was broken at the shoulder. (See Figure 24.)*

4. Range Extender Fuel Tank

The copilot seat support-structure failed, through buckling of the front legs, causing the seat to move forward. The range extender fuel tank located in this seat contacted the instrument column (see arrow, Figure 25) causing the cell to tear with its fuel (colored water) spilling over a large area. Failures of the tank were observed in the bottom and in the upper and inboard seams joining the two halves of the tank. These failures were probably due to the tank having impacted the top of the right hand window (observed in high-speed photographs).

5. Airborne Oscillograph Recording System

Examination of the airborne instrumentation recording system following the crash found this equipment to be operable. The shock absorption devices had apparently functioned to properly protect the equipment and allow its operation during the test. A study of the ground and airborne oscillograph records later showed certain discrepancies in the airborne records. (See Figure 30.)

6. Cameras

The inside side camera viewing the passenger dummy was ripped from its mounting due to collapse of fuselage structure at this location. The protective container housing this camera shielded it from damage. Moderate to good photo coverage (no internal lighting was used in this exploratory test) was obtained with three of the four airborne cameras. Good coverage was obtained with six ground cameras. (See Figure 8.)

* Also see Figure 44.

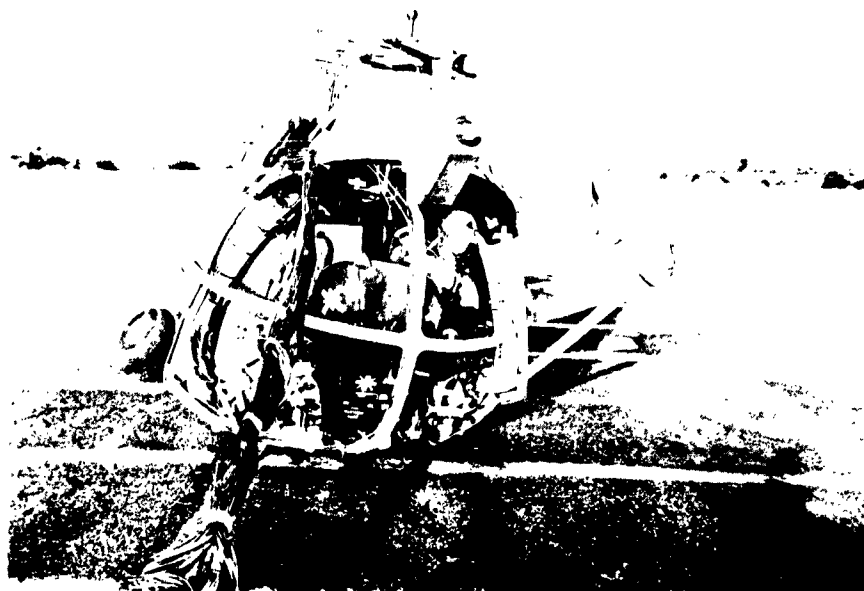


Figure 20. Post-Crash Front View

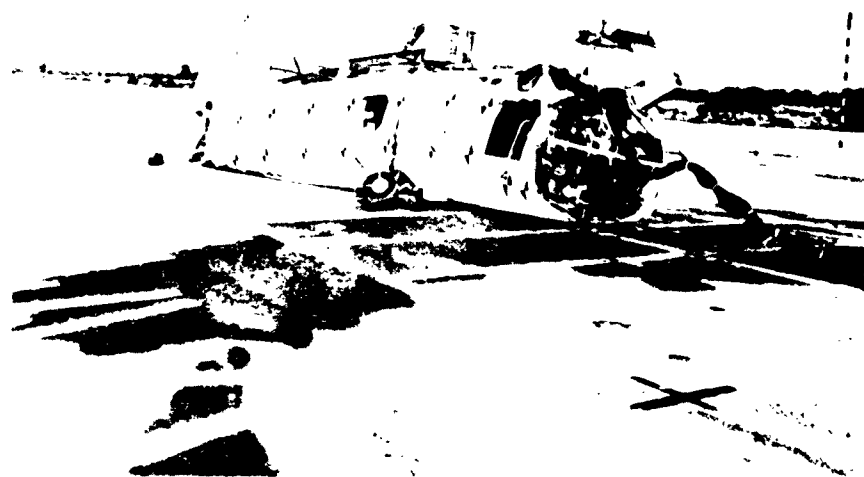


Figure 21. Post-Crash Front Quarter View

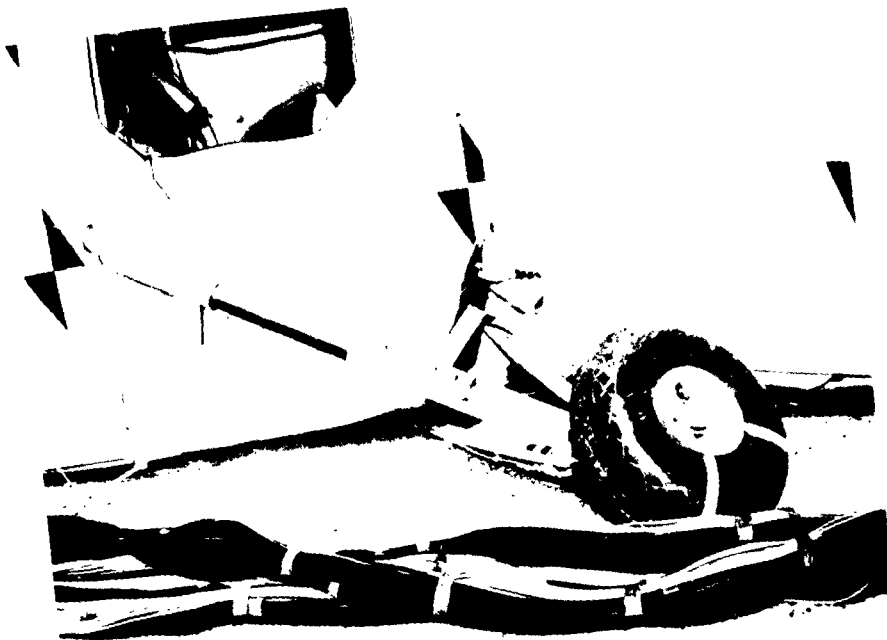


Figure 22. Post-Crash
View of Right Main
Landing Gear



Figure 23. Post-Crash View of
Dummy Pilot



Figure 24. Post-Crash View of Dummy Passenger



Figure 25. Post-Crash View of Cockpit

OSCILLOGRAPH DATA

Data Reduction

In this exploratory test no filtering was introduced between the transducers and recorders in order that maximum frequency response could be maintained. * Smoothing of the accelerometer data has thus been required as anticipated. For a discussion of the procedure used, see Appendix C. Typical original and smoothed curves are shown in Figures 26 through 29. **

Since smoothing introduces an additional source of error, the smoothed acceleration-time curves of Figures 26 through 29 were integrated to obtain velocity-time plots, providing a check on the total change in velocity of selected points of the aircraft. These curves are presented with the respective acceleration plots. In the case of the longitudinal motion of the cockpit floor, the velocity-time curve was integrated to give the displacement plot presented in Figure 29. Satisfactory agreement with the measured displacement of the aircraft (as obtained from high-speed photographs) was obtained. Reliability of the data is thus indicated.

Acceleration and Force Measurements

The acceleration-time plots and force-time plots obtained from the two crane mounted oscillographs are presented in Figures 30 through 39. Two channels of airborne recorded data (range extender tank seat-belt and shoulder-harness loads) are also shown in Figure 38. The condition of the aircraft at various times during the test is illustrated in the sequence photographs of Figure 40-1 through Figure 40-8 and may be referred to for a better understanding of events and results discussed below.

1. Comparison of Ground and Airborne Recording

A study of the ground and airborne records, particularly the comparison of the eight channels of data duplicated on these systems, has shown sufficient disagreement beyond 0.13 second

* CEC type 347 and 342 galvonometers maintain a response flat to 135 c.p.s. Natural frequency of accelerometers: 110-250 c.p.s. for 10G transducers, 850 c.p.s. for 200G units; damping 0.7 critical.

** See Appendix D for sign conventions used in all acceleration-time plots.

after impact to necessitate the temporary withholding of publication of eight channels of data recorded only on the airborne recorder. These channels are indicated in Table I and Figure 10. In Figure 30, both the original and smoothed acceleration-time curves (for ground and airborne recording) are shown for the passenger cabin floor and passenger chest accelerations. The first serious discrepancy in both cases is seen to occur at about 0.13 second. A plot of the lateral, longitudinal, and vertical accelerations of the airborne instrument package, given in Figure 31, shows that, at 0.128 second, a severe disturbance in the longitudinal acceleration record occurred. This disturbance was not a true acceleration, however, and was probably due to a poor connection at the emergency-disconnect in the umbilical cord at the crane. This disturbance at 0.128 second was clearly evident in eleven of the airborne recorder channels, although to a much lesser degree in all cases except for the fuel tank pressure record. Only minute evidence of this disturbance was observed in the other ground-recorded data.

Acceleration of the airborne package exceeded the design value of 14.5G at 0.19 second as may be observed in Figure 31. The results obtained from the airborne recorder are thus considered doubtful, pending further analysis of the data. The two channels of airborne data presented in Figure 38 (range extender tank seat belt and shoulder harness) are accurate to 0.13 second and are significant beyond this time in that the indicated loads in these belts are low.

2. Cockpit-Floor Accelerations*

Referring to Figure 32 and to the sequence photographs of Figure 40-2 and Figure 40-3, it is clear that the landing gear did not appreciably decelerate the aircraft during the impact. The 4 f. p. s. reduction in vertical velocity of the cockpit-floor, as indicated in Figure 27 for the first 0.04 second of the impact, is not borne out by a similar value for the passenger cabin floor. This value of 4 f. p. s. is within the range of experimental error for tests of this nature, and can thus be disregarded. The primary acceleration pulse began at 0.085 second, at which time the forward portion of the fuselage began to contact the ground.

* See Appendix D for sign conventions.

In a rise time of 0.017 second the vertical acceleration peaked at 115G. * The relatively high stiffness of the forward fuselage ring and the small distance between floor and the bottom of the aircraft (allowing little deceleration distance) would account for the high peak vertical acceleration and high rate of onset at this point compared to the passenger cabin floor (discussed in the following section).

The longitudinal acceleration of the cockpit floor (Figure 32) builds up gradually to about 20G at 0.09 second due to the gradually increasing contact area between the fuselage and ground. (See Figures 40-2 and 40-3.) The sudden reduction to zero G's at 0.10 second is probably attributable to the rapid breaking up of the floor structure (115G vertical acceleration at 0.105 second) in the immediate vicinity of the accelerometer attachment point, ** thus momentarily relieving the longitudinal forces at this part of the aircraft. A 45G peak longitudinal acceleration followed immediately.

The positive longitudinal accelerations from 0.12 to 0.19 second represent an increase in the forward velocity of this portion of the aircraft in this interval (Figure 29), and is associated with the relieving of longitudinal compressive stresses in the lower air-frame structure at this time. This follows since there is evidence of the tendency of the aircraft to "float" over the surface during this interval, i. e., near zero vertical accelerations in the interval and a second minor impact occurring at 0.47 second (not shown). The film obtained from Camera No. 7G, Figure 8, (200 frames per second) clearly shows this increase in forward velocity of the cockpit area in the interval 0.12 to 0.19 second.

The lateral acceleration of the cockpit floor was of an oscillatory nature with peaks of 10G to 15G and a frequency (irregular) of the order of 20 cycles per second, with corresponding amplitudes of about 1/4-inch.

3. Passenger Cabin Floor Accelerations

In general, the pattern of accelerations at the passenger cabin floor level follows that for the pilot compartment. Almost no (2.5 f. p. s.) reduction in the vertical velocity was attributable to the action of the landing gear up to the time of its failure at 0.05 second. (See Figures 26 and 40-3.) The vertical acceleration built up slowly as compared to that for the pilot compartment

* Maximum probable error on peak accelerations quoted in this report are estimated at 15 percent.

** As found from post-crash inspection.

and reached a peak value of 61G at 0.10 second or about 5 milliseconds earlier than for the corresponding 115G peak value for the cockpit floor. That the time delay should exist is made obvious from a study of the sequence photographs of Figure 40, i. e., the aircraft first contacted the ground at the tail section, then settled progressively along the longitudinal axis toward the nose section. The lower peak vertical acceleration at the passenger cabin floor, as compared to the pilot compartment, was probably due in part to the decrease in vertical stiffness of the floor support-structure in the area of the landing gear attachments caused by the earlier failure of these attachments and the structure with the gear. (See Figure 22. *) The peak longitudinal acceleration, 36G, was of the same order of magnitude as for the passenger cabin floor.

4. Pilot Harness Loads and Pelvic Accelerations **

A study of Figure 34 shows that the peak longitudinal and vertical accelerations observed at the floor level were carried through to the pilot dummy pelvic-region with a time delay of approximately 10 milliseconds. There was, approximately, a 50 percent reduction in amplitude of the main pulse in each case, but with a corresponding increase in time duration as would be anticipated. In fact, the pelvic vertical acceleration was maintained at an average value of about 30G for some 0.040 second, accounting for a change in velocity of 39 f. p. s. in this interval.

Film records from cameras 1A and 2A (Figures 2 and 11) indicate that the pilot seat started to fail (rotate about rear floor attachments) at 0.11 second. A post crash inspection showed this to be due to the buckling of both front legs of the tubular steel seat.

The time of failure is seen from Figure 34 to correspond with a sudden reduction of load in the shoulder harness (as would be expected since the shoulder harness is attached to the seat structure in the H-25A aircraft) and with the peak pelvic vertical acceleration 60G. The seat continued to rotate (Figure 41) until 0.143 second, at which time a very abrupt reduction in the forward

* Also see discussion of cockpit floor accelerations, page 37.

** It must be emphasized that all accelerations recorded within the dummy pilot and passenger are simply the responses of the dummy structure, in many respects dissimilar to the human frame, to the input accelerations to the dummy. Direct correlation of these accelerations with those that would be experienced by a human occupant is questionable. Orders of magnitude and event timing are probably representative of an actual crash, however.

velocity of the seat and dummy with respect to the aircraft is shown by camera No. 2A (Figure 11). The 40G vertical and 43G longitudinal pelvic accelerations of Figure 34, occurring at 0.143 second, are thus in agreement with the hi-speed photographic record, as are the peak lateral and longitudinal chest accelerations of Figure 35.*

Stoppage of the forward motion of the seat is attributable to these sources:

- a. Contact of the pilot's head with the main fuselage frame in the region of the pilot compartment. (See Figure 41.)
- b. Contact of the forward edge and bottom of the pilot seat with the underlying structure, i. e., floor and control system. (See Figure 25.)
- c. Forces transmitted to the pilot dummy through the legs. (See Figure 42.) Note the evidence of high loads as shown in the photograph, and note that the right hand foot was pushed under or around (questionable) the right hand pedal.

It is of considerable interest that the shoulder harness and seat belt loads were extremely low in comparison to the mass-acceleration product for the pilot dummy anatomical components. It is thus obvious that these forces were negligible compared to the other forces transmitted to the pilot torso through the legs, seat, and fuselage frame.

5. Pilot Chest Accelerations

As in the case of the pelvic accelerations, the chest accelerations for the pilot dummy initially correspond fairly closely with the accelerations of the cockpit floor. (See Figure 35.) It is of interest that the initial peak chest longitudinal acceleration (27G) while lagging that for the floor, slightly leads that of the pelvic region. The 14G lateral chest acceleration is associated with the abrupt stoppage of the forward motion of the pilot and seat as discussed in the preceding paragraph.

* Records for the pilot head also show 80G longitudinal and 12G lateral (10G range accelerometer bottomed) at this time. Because these records were obtained on the airborne oscillograph and are of questionable accuracy, they have been omitted from this report.

Progressive attenuation of the vertical accelerations from the floor upward appears to have existed as shown by these recorded values:

Floor	115G
Pelvic Region	60G
Chest Region	51G
Head (Obtained from airborne oscillograph)	45G

Such attenuation is not necessarily always found in the impact of elastic systems. In fact, amplification is often discovered.*

6. Passenger Seat Belt Load and Chest Accelerations

A comparison of the accelerations for the passenger dummy with the corresponding seat belt loads (Figures 24 and 36**) illustrates, as in the case of the pilot dummy, that the seat belt load was relatively low (1,100 pounds maximum***) compared to the loads from other sources. For the passenger, these loads came from:

- a. the troop seat,
- b. the floor of the aircraft, and
- c. the left wall of the aircraft.

The film record from hi-speed camera No. 4 shows that at 0.105 second the passenger, while sitting essentially upright, started to move downward with respect to the aircraft. At 0.15 second this motion was abruptly halted. These times are noted in Figure 36 and correspond to: (1) the failure of the seat at 13G, and (2) contact of the dummy while in a sitting position with the floor of the aircraft, giving a peak acceleration of 56G. The peak

* Robert R. Luke, "The Impact Responses of a Single-Degree-of-Freedom System With Viscous Damping", The University of Texas Structural Mechanics Research Laboratory, Austin, Texas, June 16, 1960.

Albert P. Richter, Jr., "The Response of a Two-Degree-of-Freedom Undamped System Subjected to Impulsive Loading", The University of Texas Structural Mechanics Research Laboratory, Austin, Texas, August 1960.

** See Appendix D for sign conventions.

*** The belt did not fail.

lateral and longitudinal accelerations and seat belt load will be seen from Figure 36 to occur at or near the time (approximately 0.15 second after impact) at which the passenger dummy contacted the floor.

7. Passenger Head Accelerations

During the interval 0.105 to 0.150 second, the vertical axis through the passenger dummy's head was observed to rotate clockwise, as seen in Figure 3, through approximately 50 degrees. Thus, the "vertical" and "longitudinal" accelerations presented in Figure 37 are not so aligned with respect to the airframe, but with respect to the rotated head.* Thus, the peak (56G) vertical acceleration recorded in the dummy chest region upon impact of the dummy with the floor, following the seat failure, should have been transmitted to the head with considerable reduction in magnitude. Thirty-three G's were recorded, as seen in Figure 37; further, the peak "vertical" head acceleration occurred simultaneously with the peak vertical chest acceleration. The rotation of the head from the vertical should also have resulted in positive "longitudinal" accelerations in the head for negative vertical accelerations in the chest.** A sharp positive peak "longitudinal" acceleration of 11G is seen from the figure to exist in conjunction with the primary vertical pulse due to the impact with the floor. Actually, the true peak was probably higher than 11G; however, the 10G range accelerometer used has since been shown on bench test to bottom at about -11G and +13G, and probably did bottom on this short duration pulse without presenting visible evidence of such bottoming. There is no question but that the accelerometer did bottom on the subsequent two negative pulses as shown in Figure 37. The high-speed photographs show a rapid deceleration of the forward rotation of the head in this period which account for these large negative "longitudinal" values.

The lateral head acceleration consisted of two pulses. The first was an 80G deceleration at 0.165 second, i. e., immediately following the vertical impact of the dummy with the floor. This was followed by 22G acceleration at 0.21 second. The velocity changes corresponding to these pulses were -37 f. p. s. and +10 f. p. s., respectively. These motions are not visible in the high-speed photographs because of the motion of the aircraft

* Observe from Appendix D that the "longitudinal" direction of the dummy is the lateral direction with respect to the airframe itself.

** Neglecting elasticity of the dummy.

itself and because these motions* were along the line of sight of the camera.

8. Range Extender Tank Loads

The seat belt and shoulder harness loads were, as for the pilot, relatively low. (See Figure 38.) They remained below 970 pounds and 300 pounds, respectively, building to or near these values as the longitudinal acceleration of the cockpit floor began to build up. Observation of the upper portion of the seat through high-speed camera No. 1A indicated that the collapse of the seat began at 0.11 second, i. e., at or near the time for the peak accelerations of the cockpit floor. This time was the same as that for the failure of the pilot seat. Buckling of the forward legs of the seat allowed the seat to rotate and move forward. At 0.145 second the forward inboard corner of the tank contacted the instrument console (Figures 25 and 43) rupturing the fibre-glass tank, and fuel spillage began. Other tank failures were: (1) failure in the pan area of the seat (a cushion was placed between tank and seat), and (2) separation of the upper and inboard seams due to contact of the filler cap with the top window-sill of the right hand window of the aircraft.

* The total displacement of the head with respect to the airframe during the 27 milliseconds required for the 37 f. p. s. velocity change would only be about 2 inches.

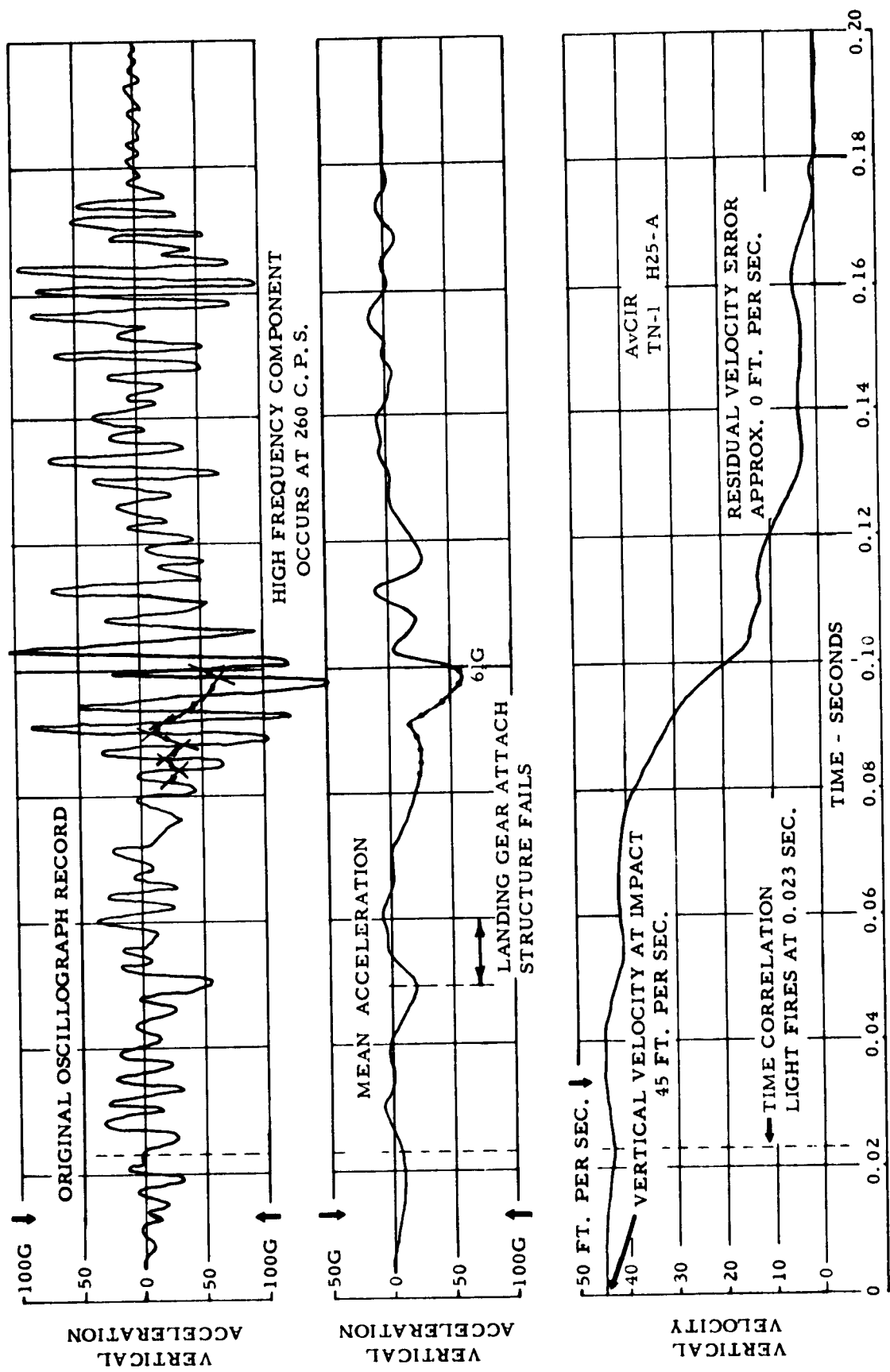


Figure 26. Acceleration and Velocity of Passenger Cabin Floor

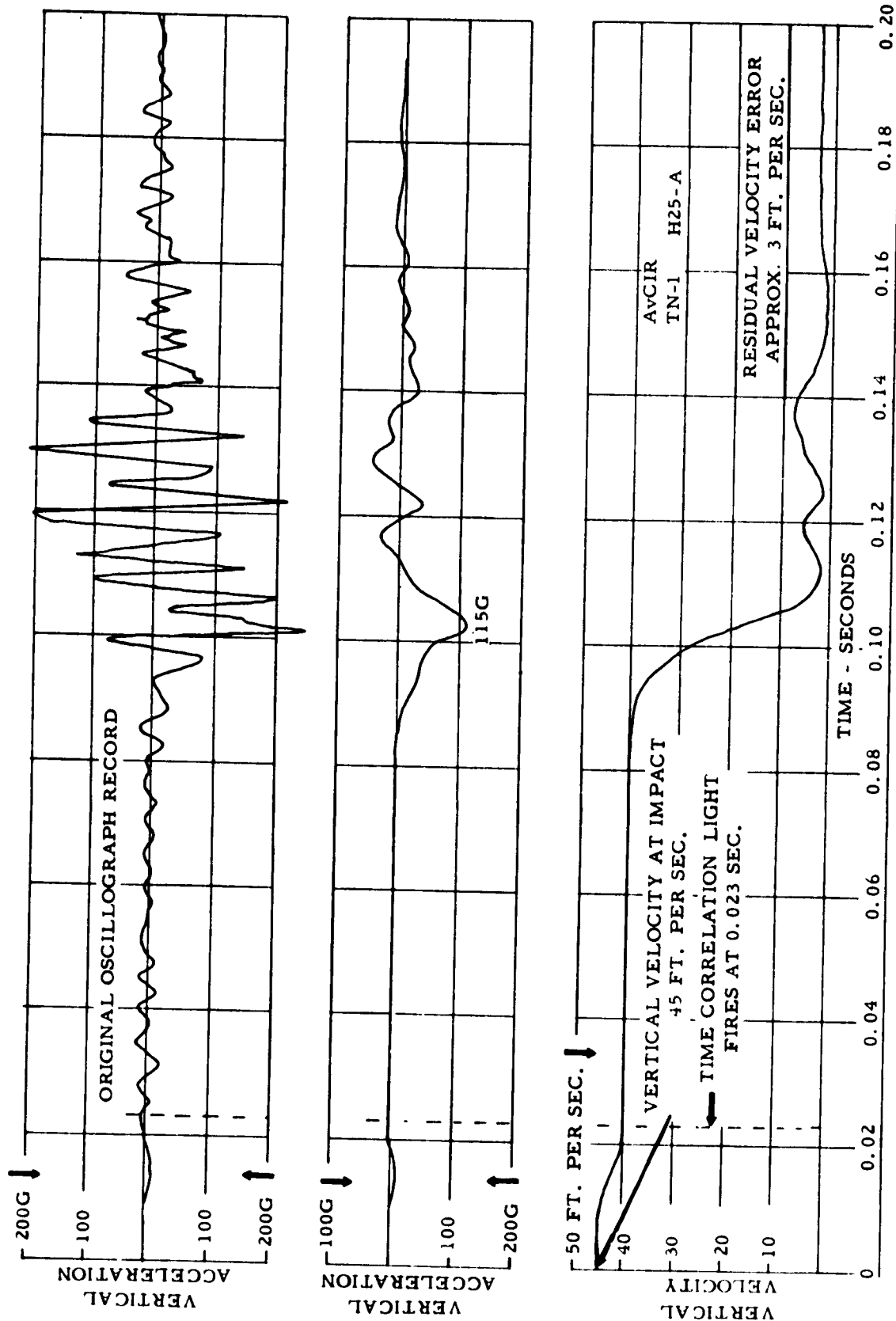


Figure 27. Acceleration and Velocity of Cockpit Floor

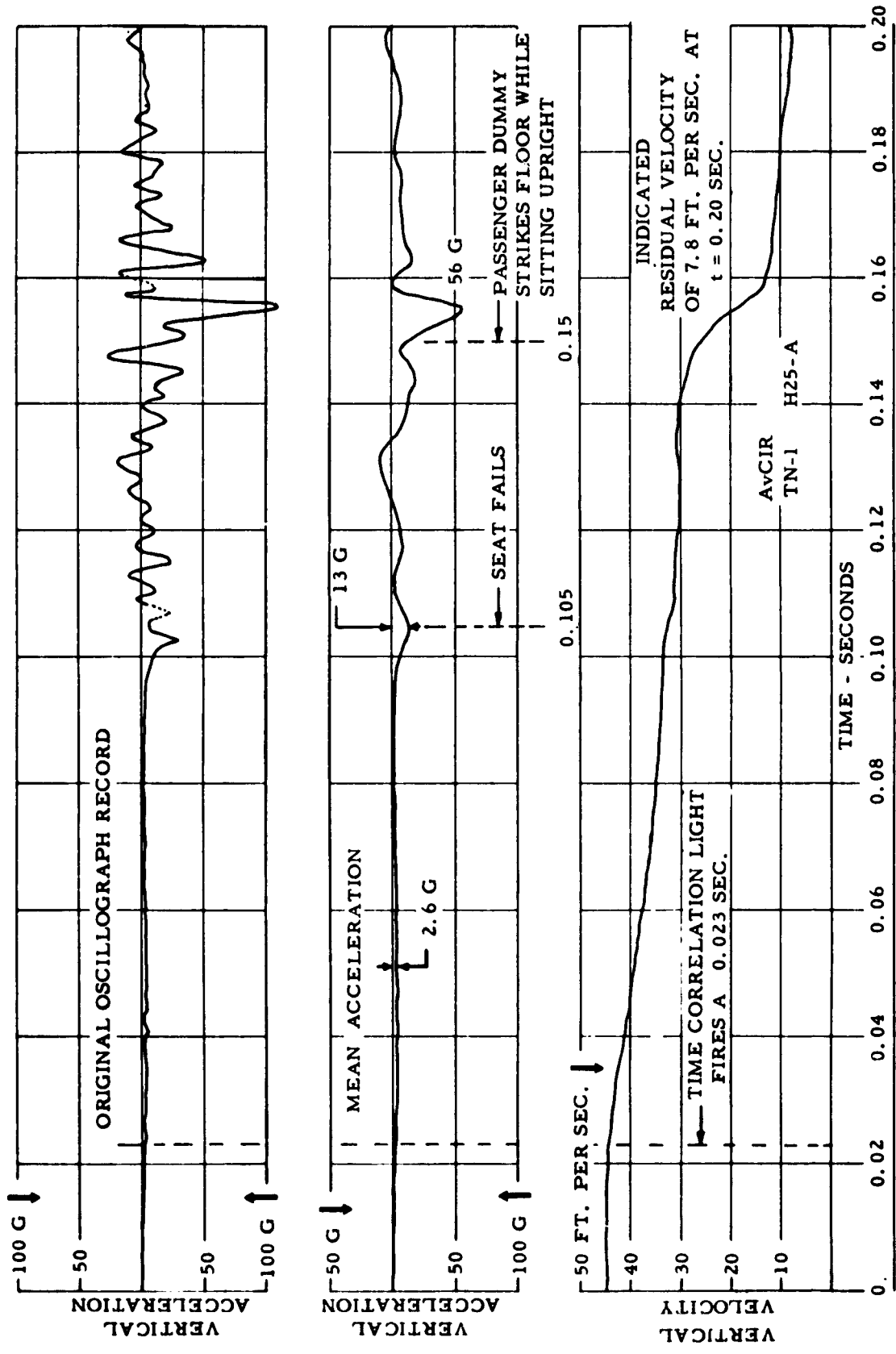


Figure 28. Acceleration and Velocity of Passenger Chest

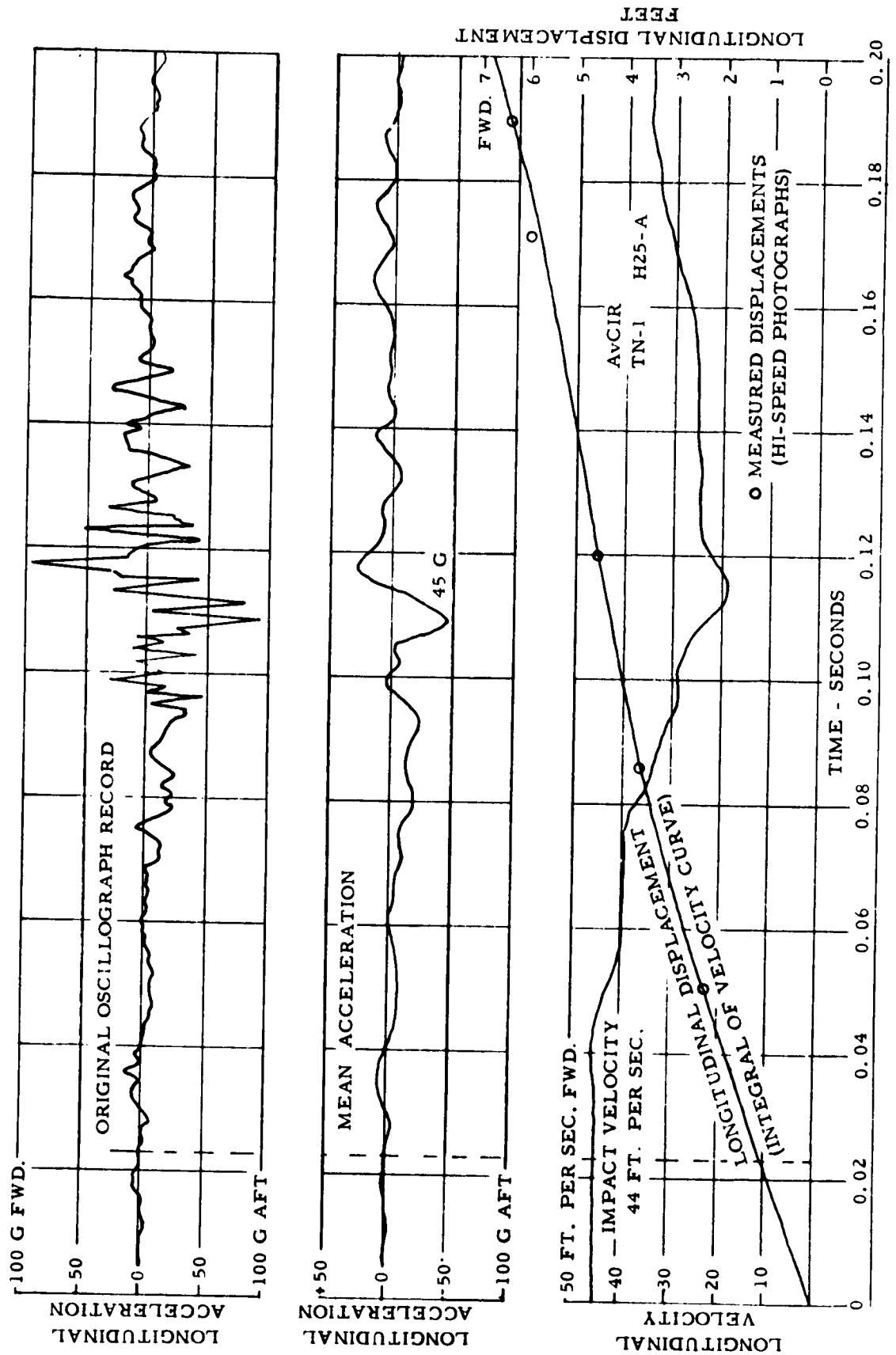


Figure 29. Acceleration, Velocity, and Displacement of Cockpit Floor

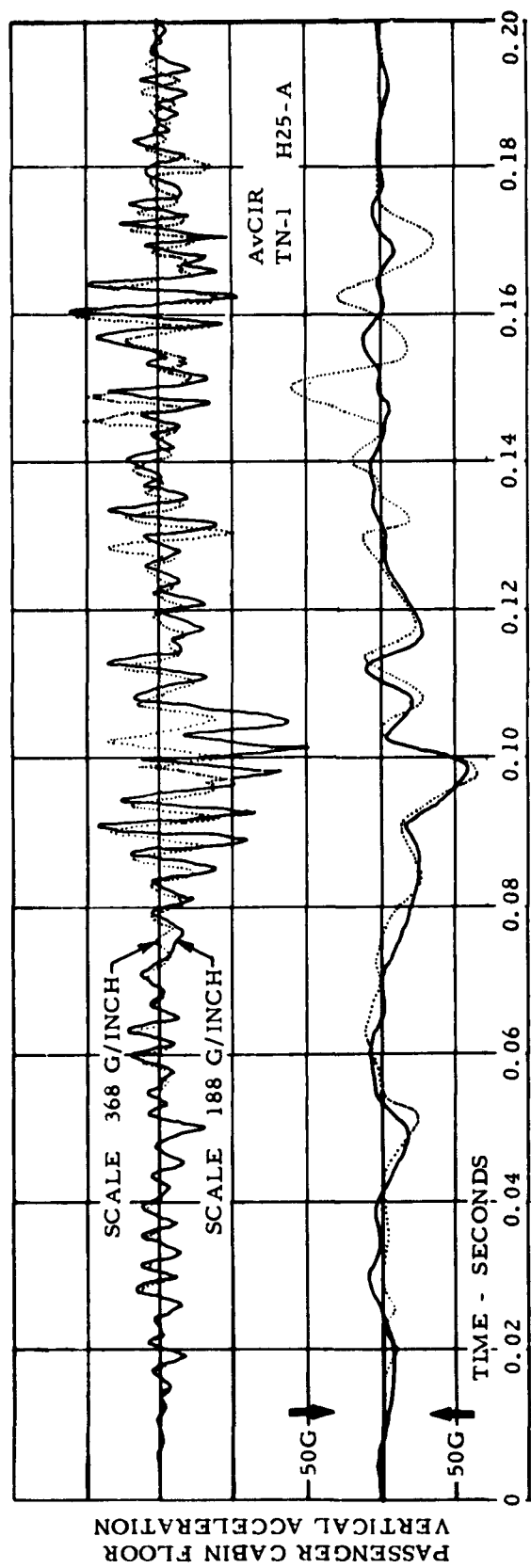
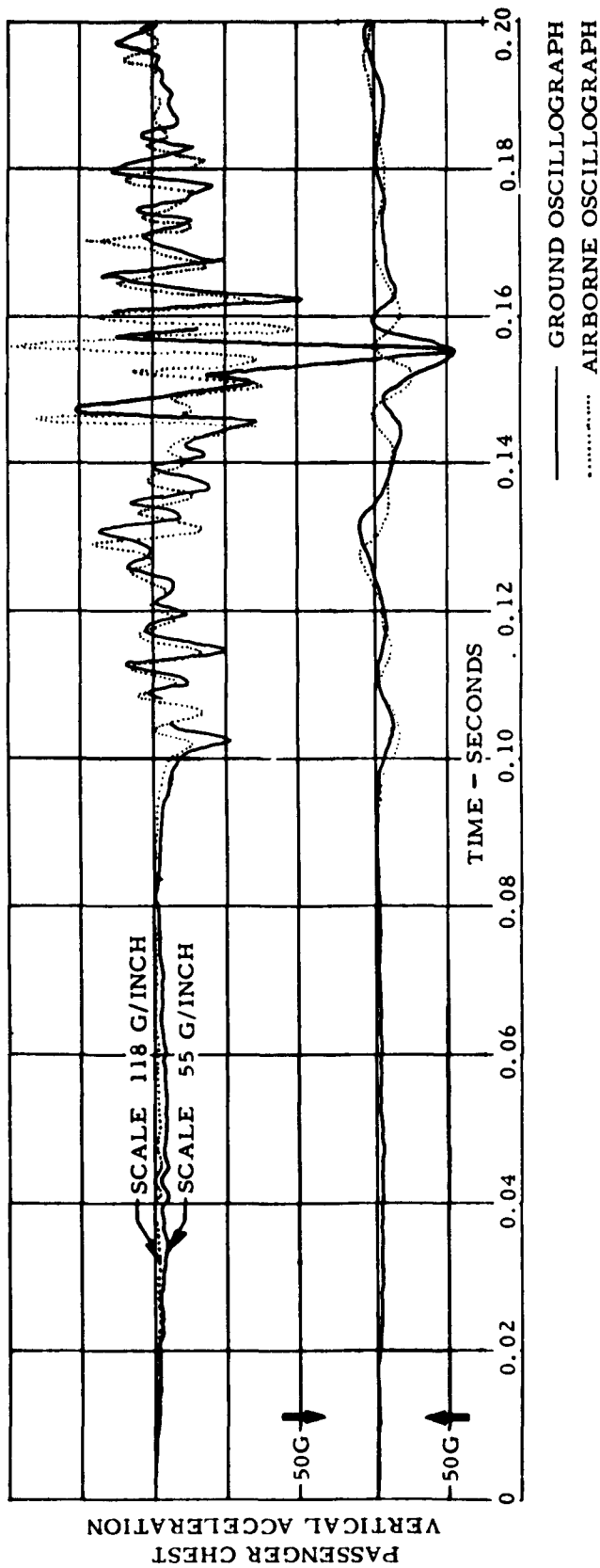


Figure 30. Comparison of Ground and Airborne Recording

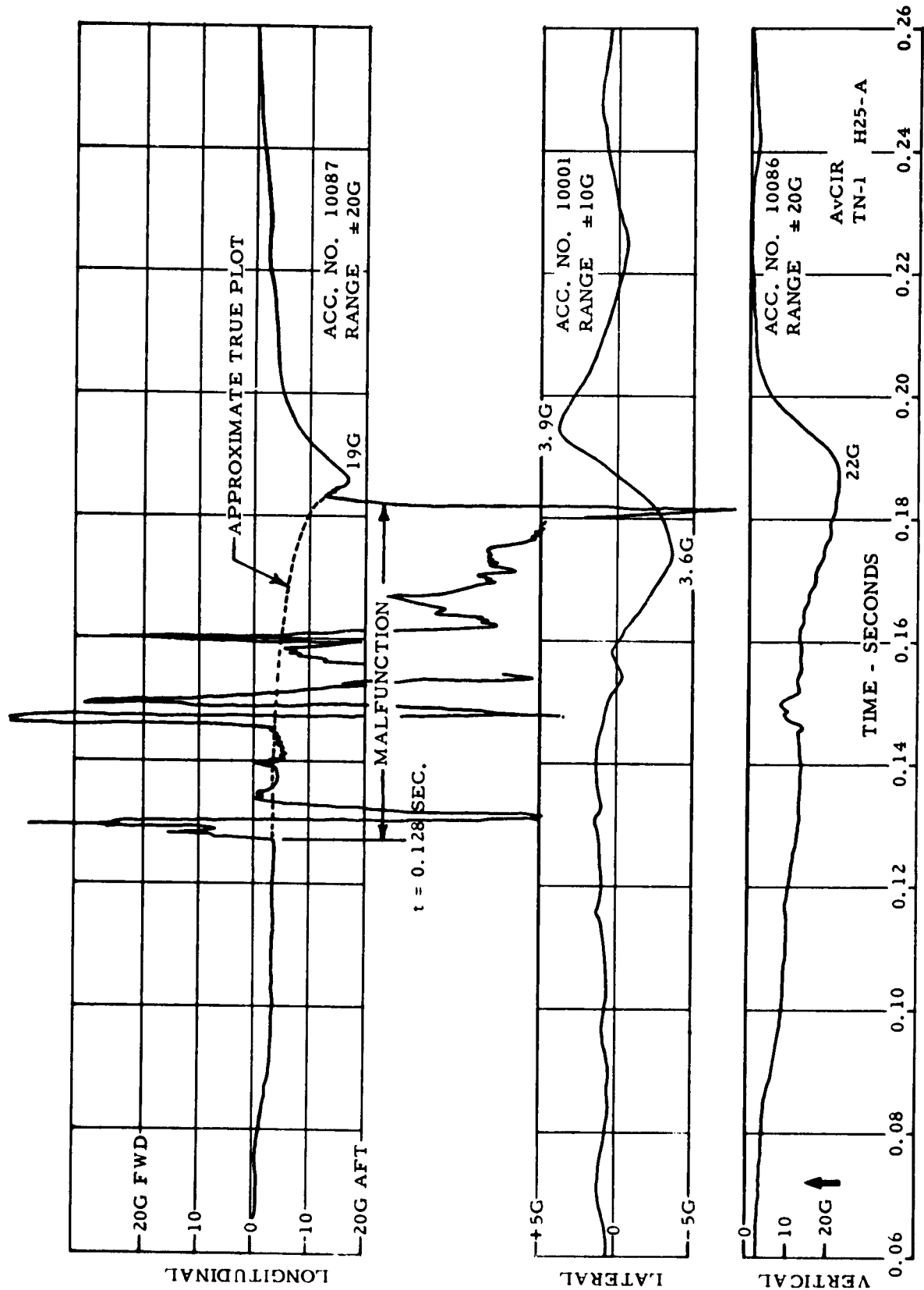


Figure 31. Accelerations of Airborne Instrument Package

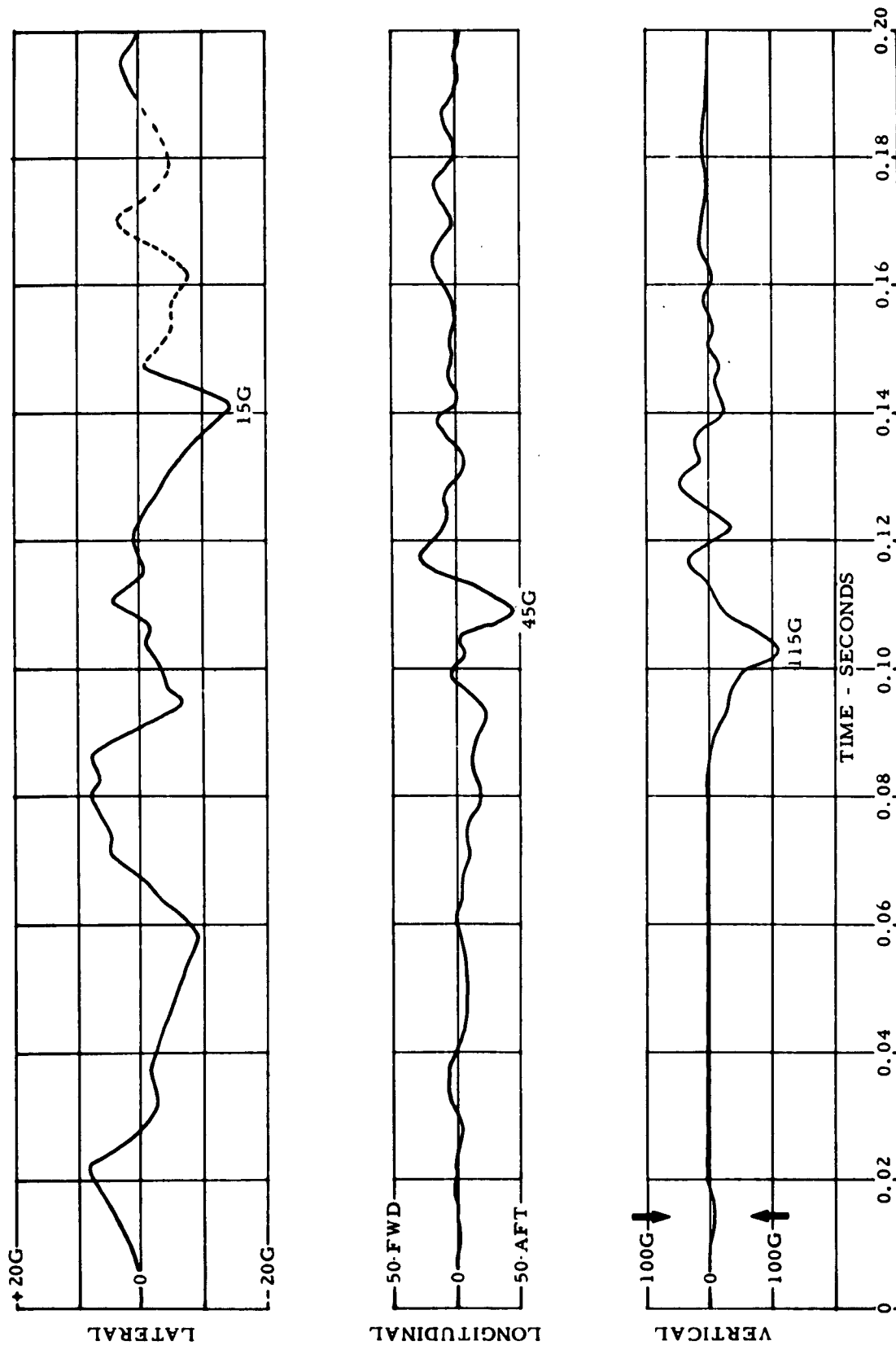


Figure 32. Cockpit Floor Accelerations

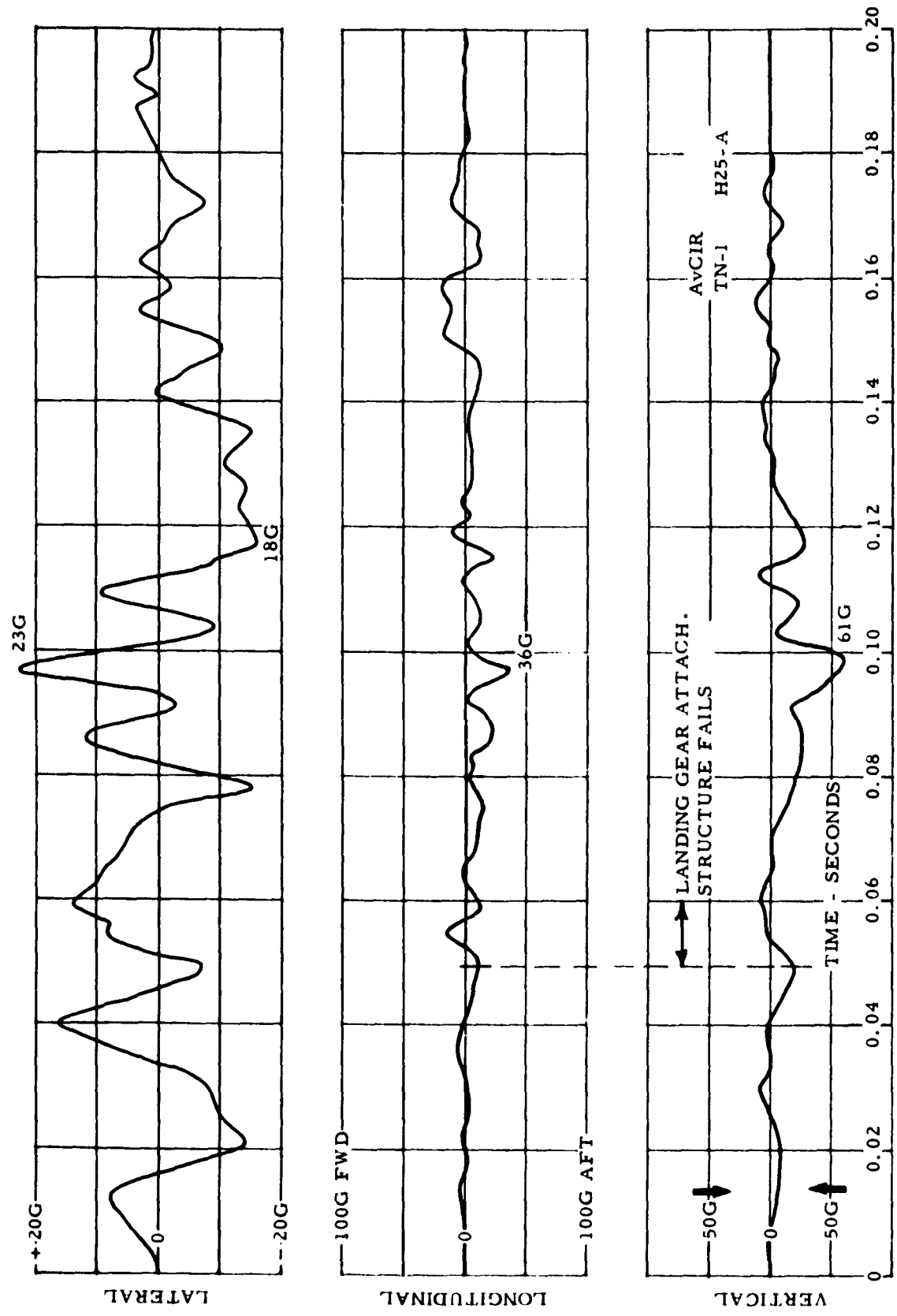


Figure 33. Passenger Cabin Floor Acceleration

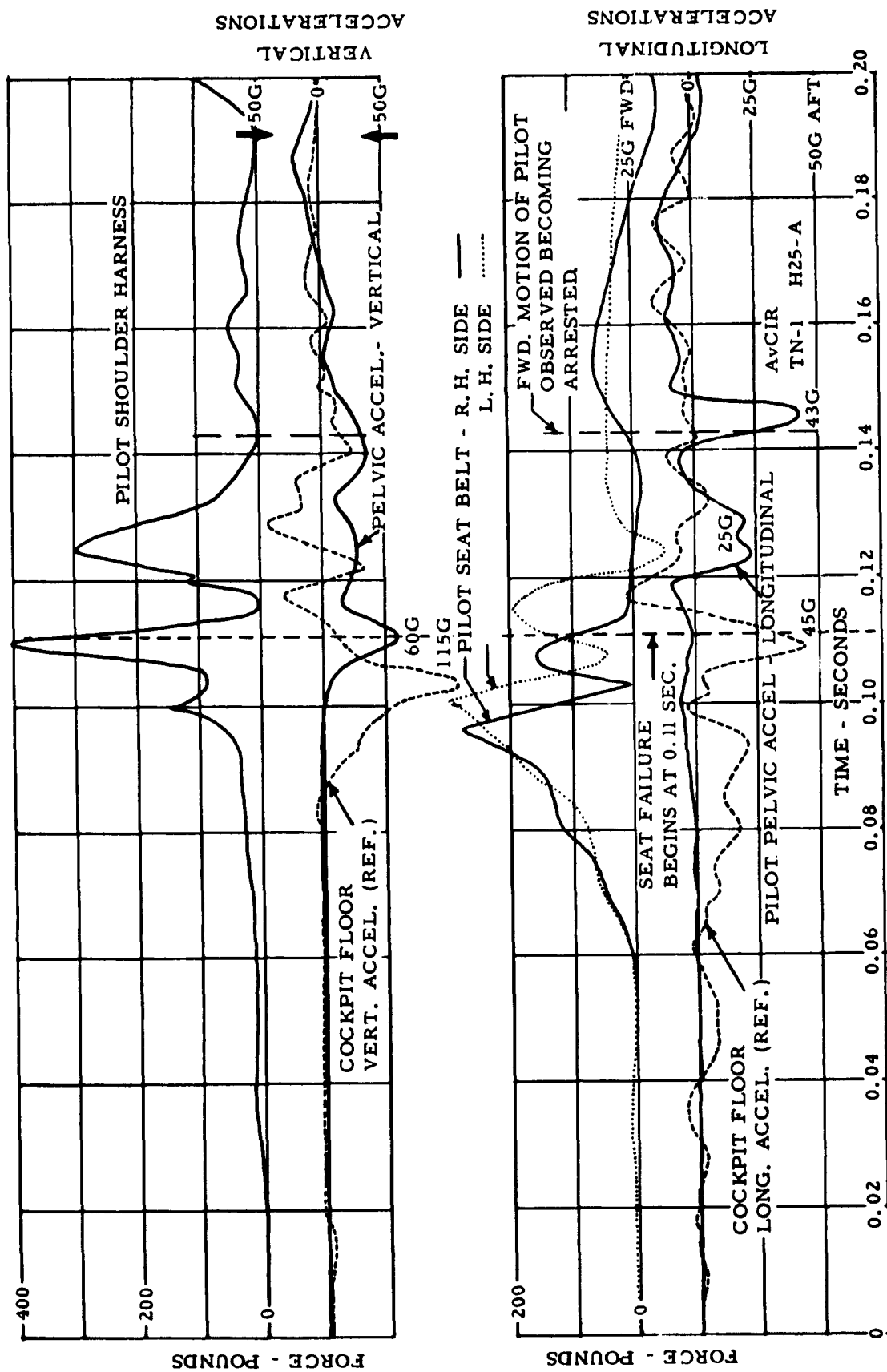


Figure 34. Pilot Shoulder Harness and Seat Belt Loads and Pelvic Accelerations

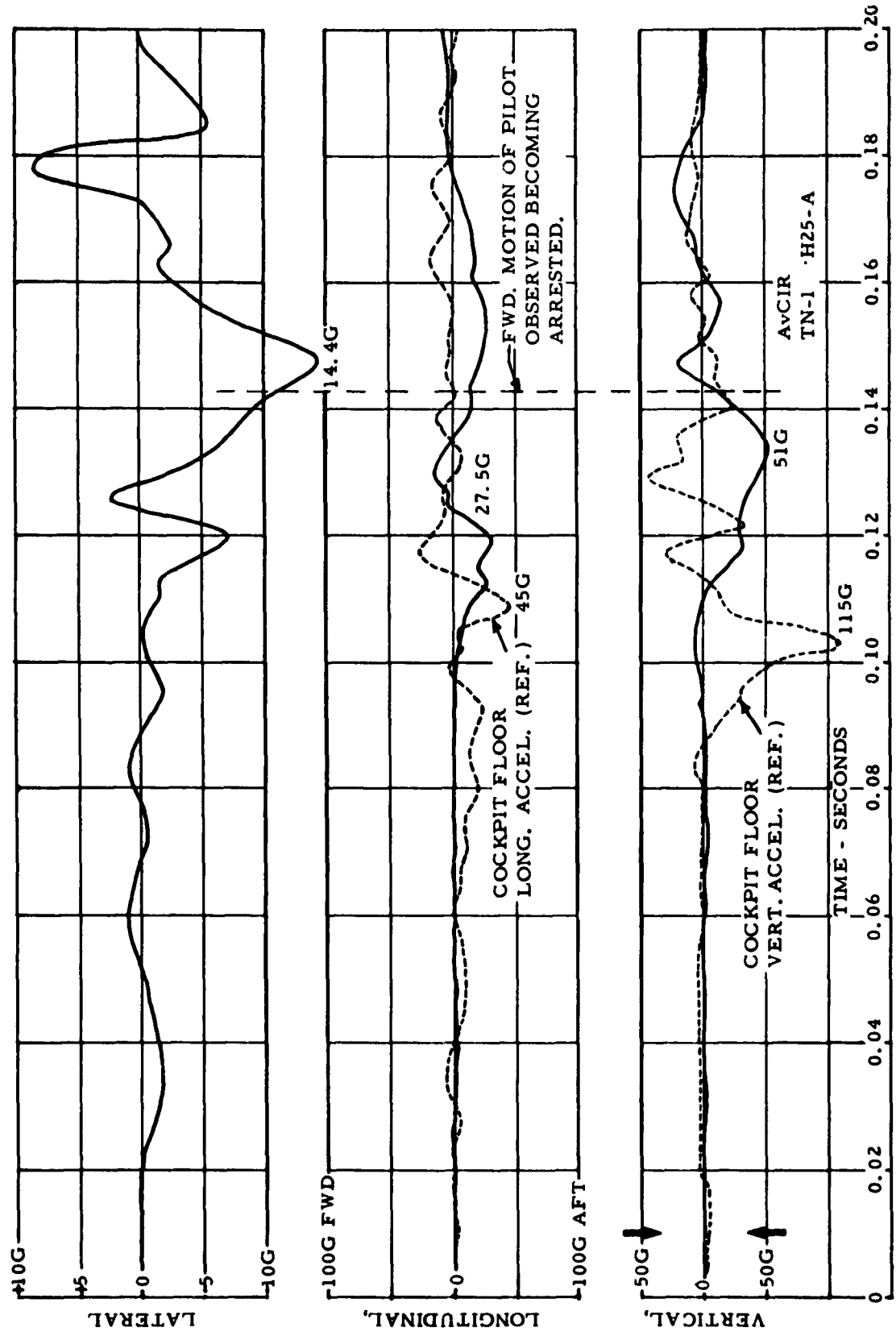


Figure 35. Pilot Chest Accelerations

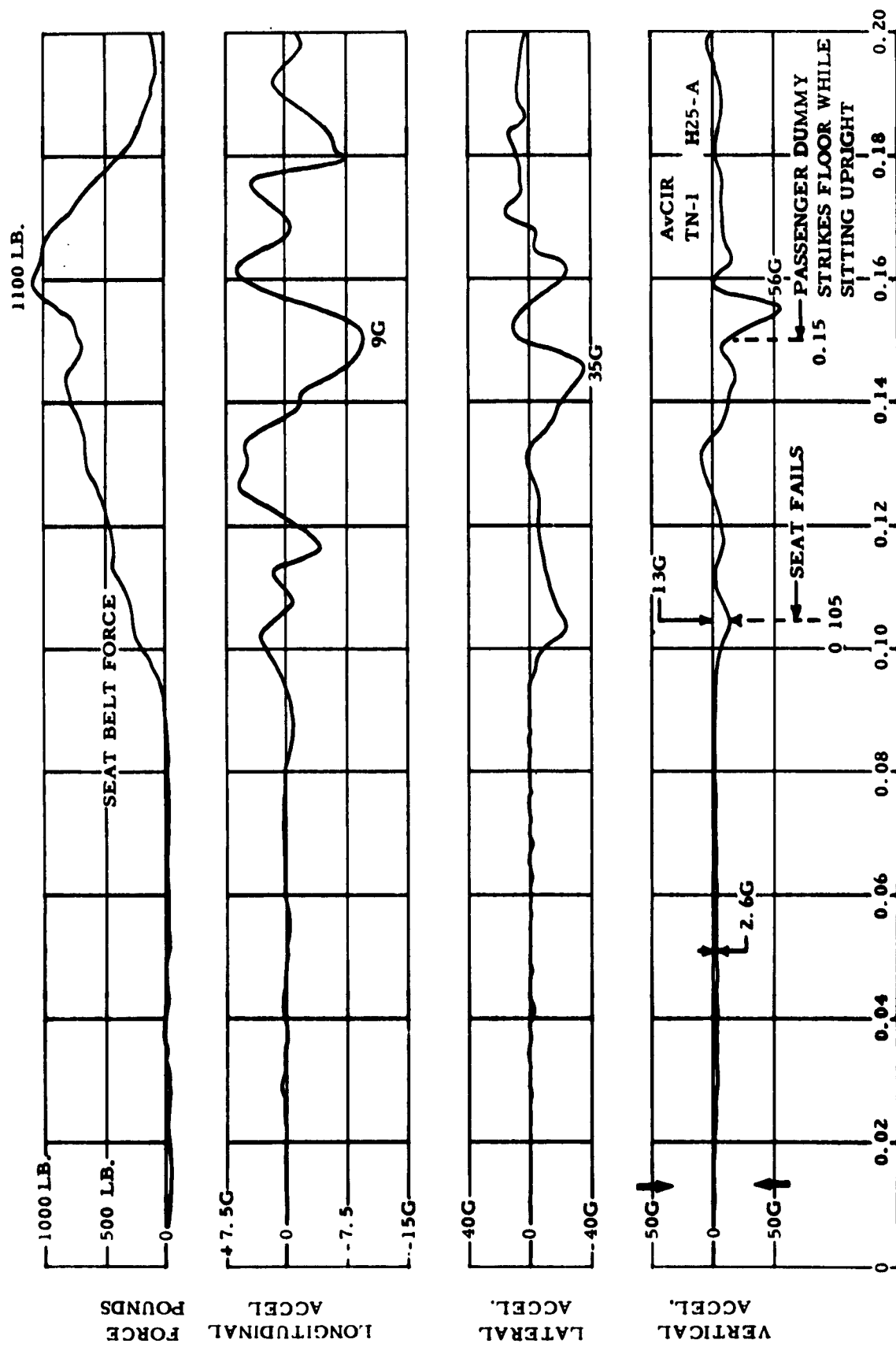


Figure 36. Passenger Seat Belt Loads and Chest Accelerations

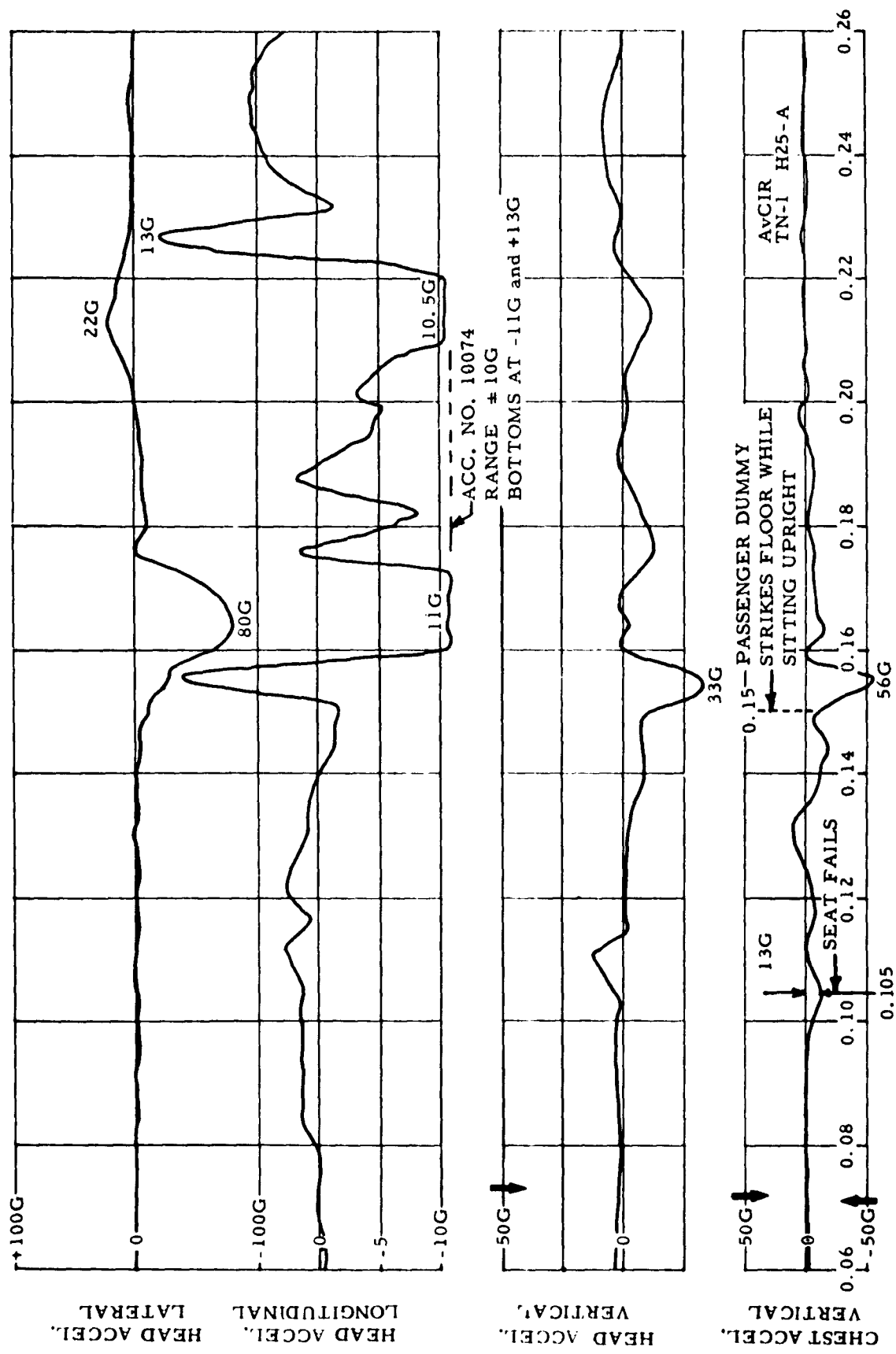


Figure 37. Passenger Head Accelerations

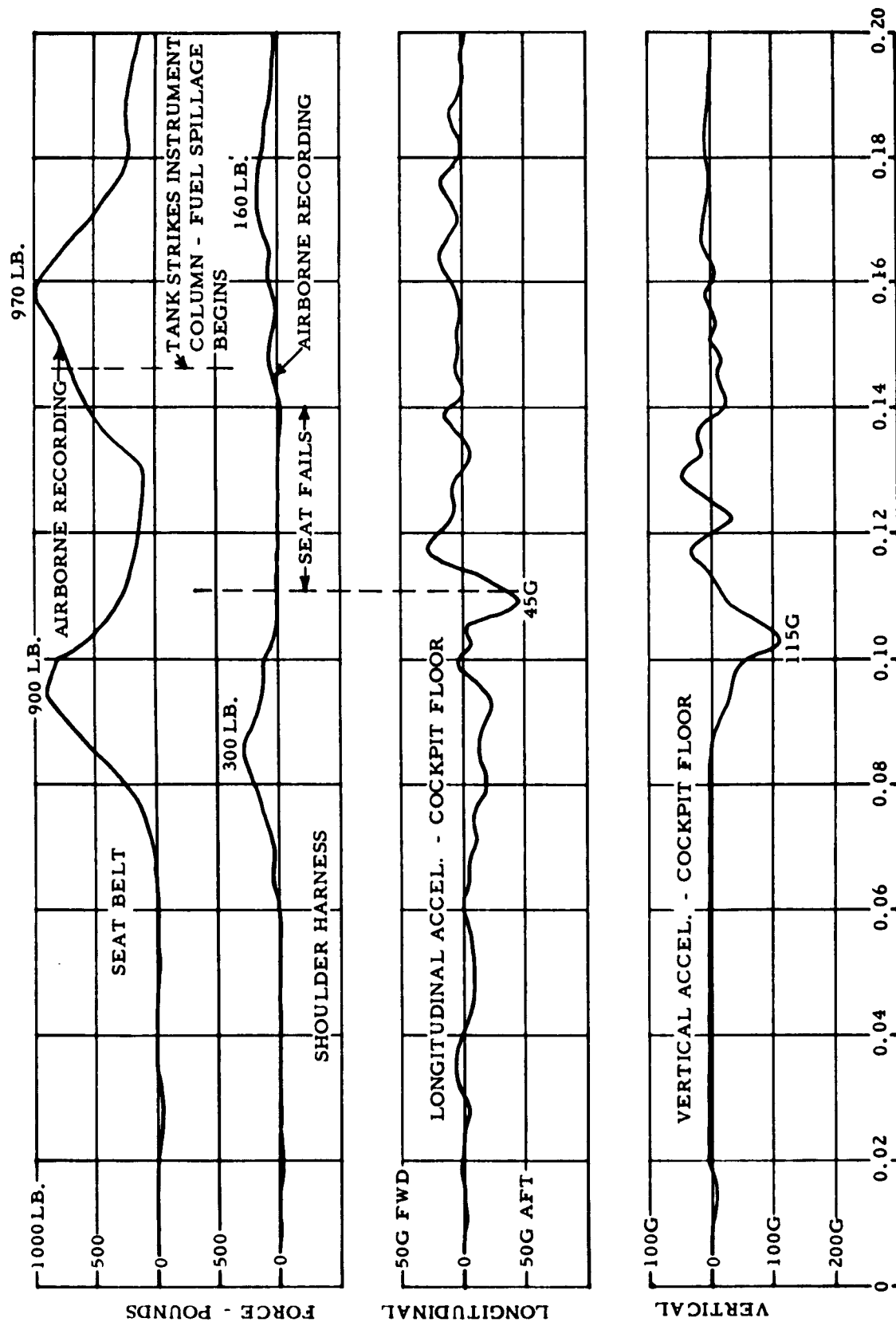


Figure 38. Range Extender Tank Loads

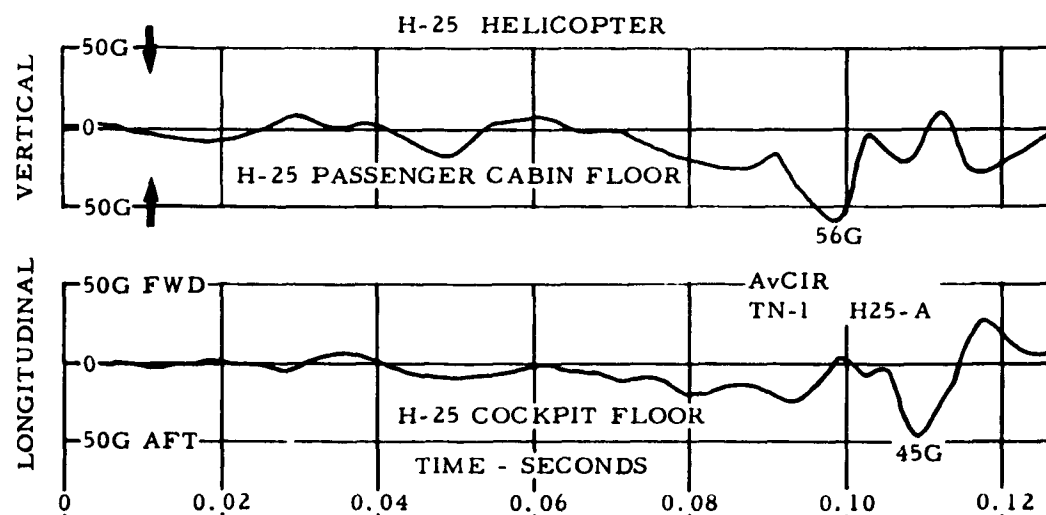
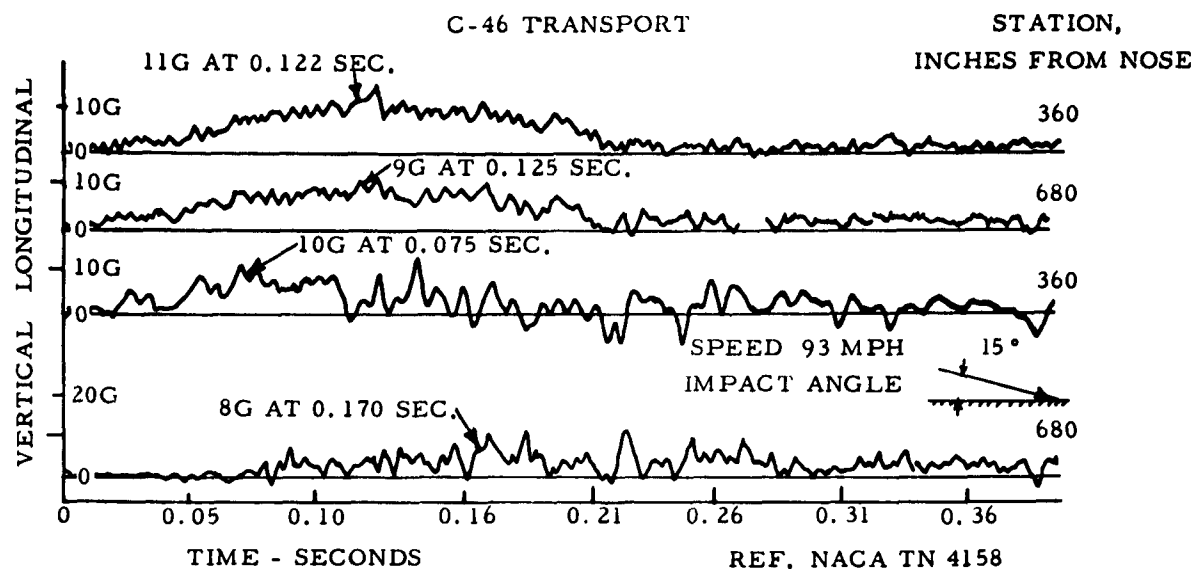


Figure 39. Comparison of Horizontal and Vertical Accelerations for a C-46 Transport and an H-25A Helicopter

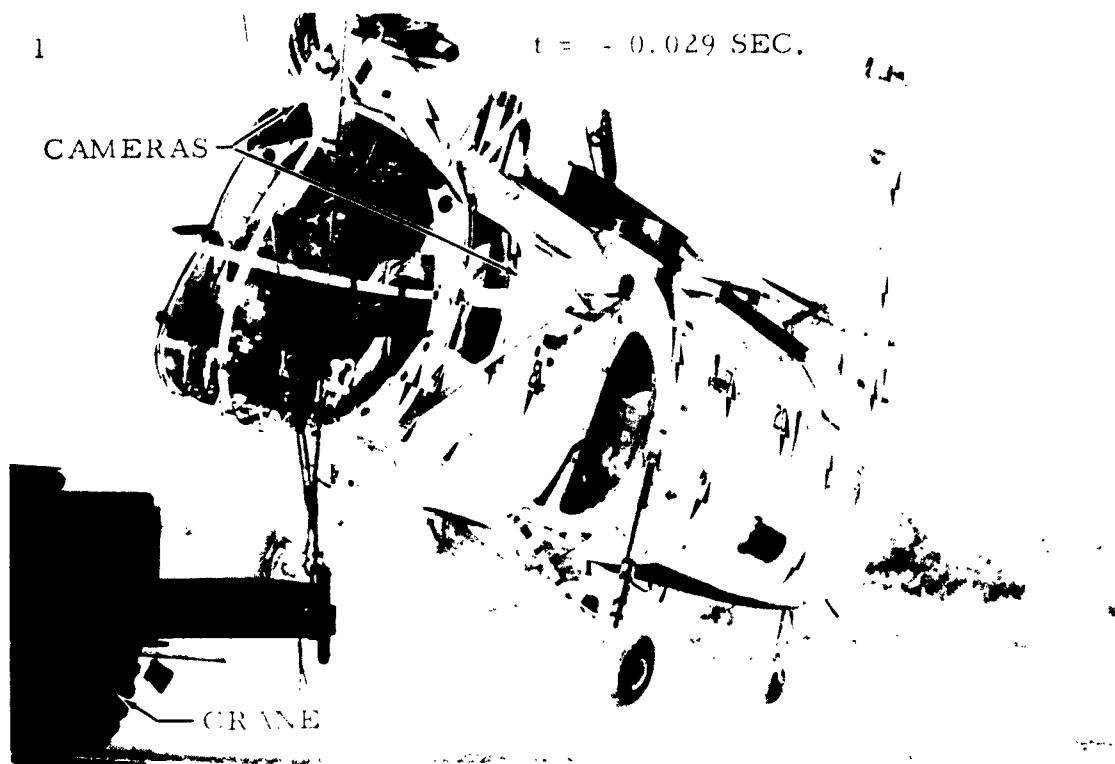


Figure 40-1. Sequence Photograph, H-25 Drop Test

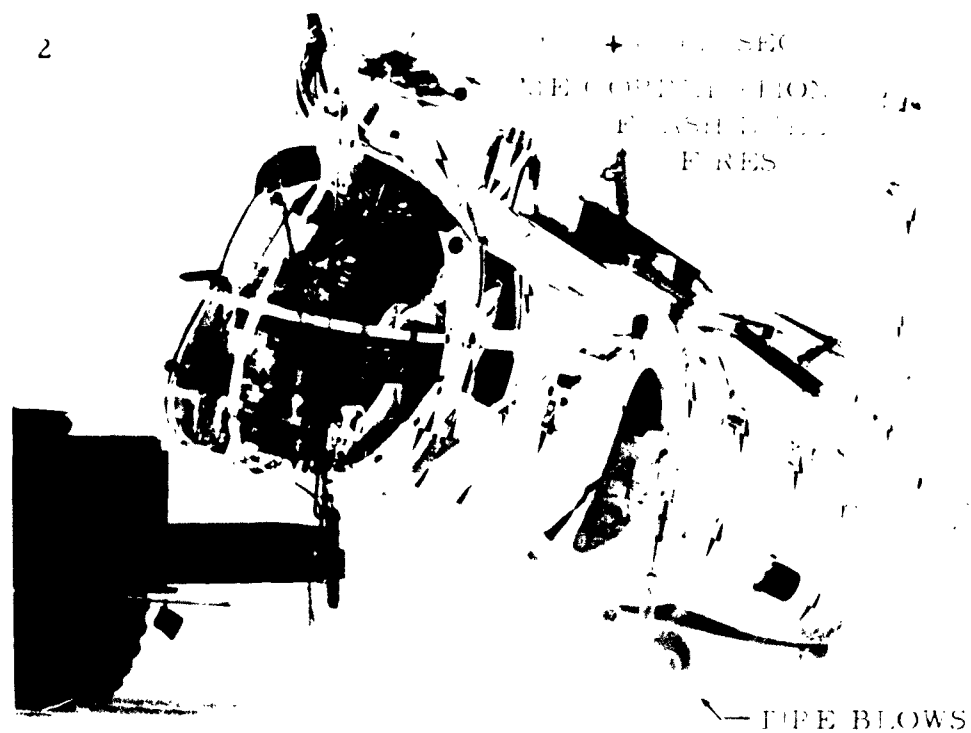
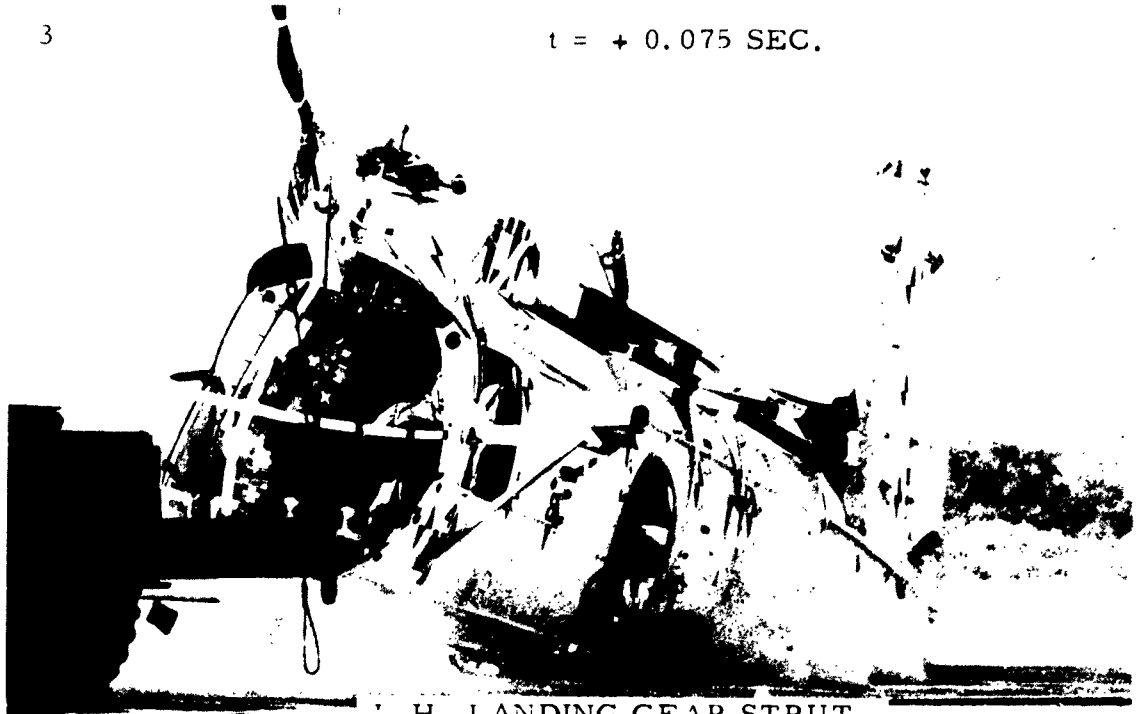


Figure 40-2. Sequence Photograph, H-25 Drop Test

3

$t = + 0.075 \text{ SEC.}$



L. H. LANDING GEAR STRUT
PUSHES THROUGH FUSELAGE

Figure 40-3. Sequence Photograph, H-25 Drop Test

4

$t = + 0.127 \text{ SEC.}$

FORWARD UNDER-BELLY BEGINS
TO CRUSH, MOVING PILOT'S KNEES
AND FEET FORWARD WITH RESPECT
TO TORSO

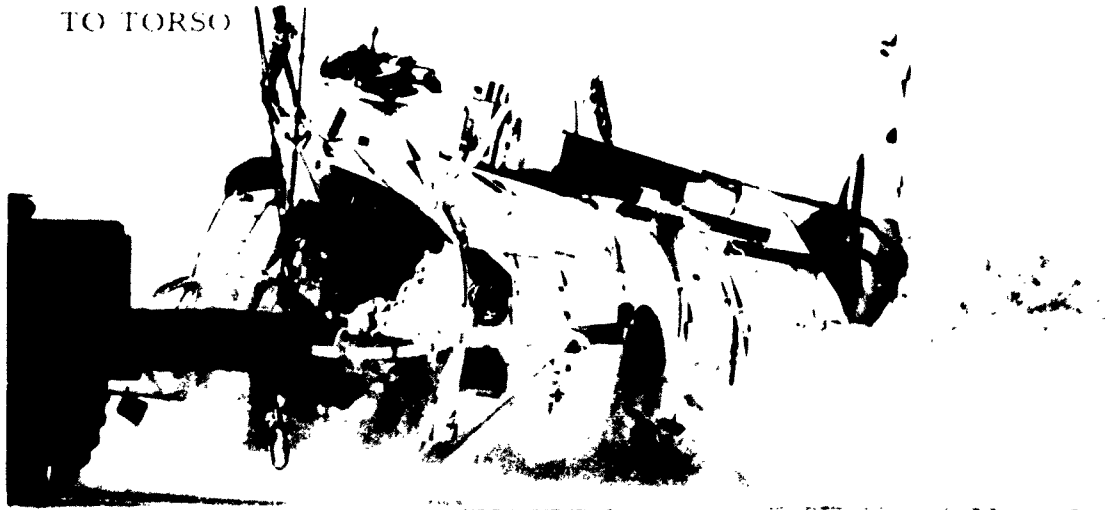


Figure 40-4. Sequence Photograph, H-25 Drop Test

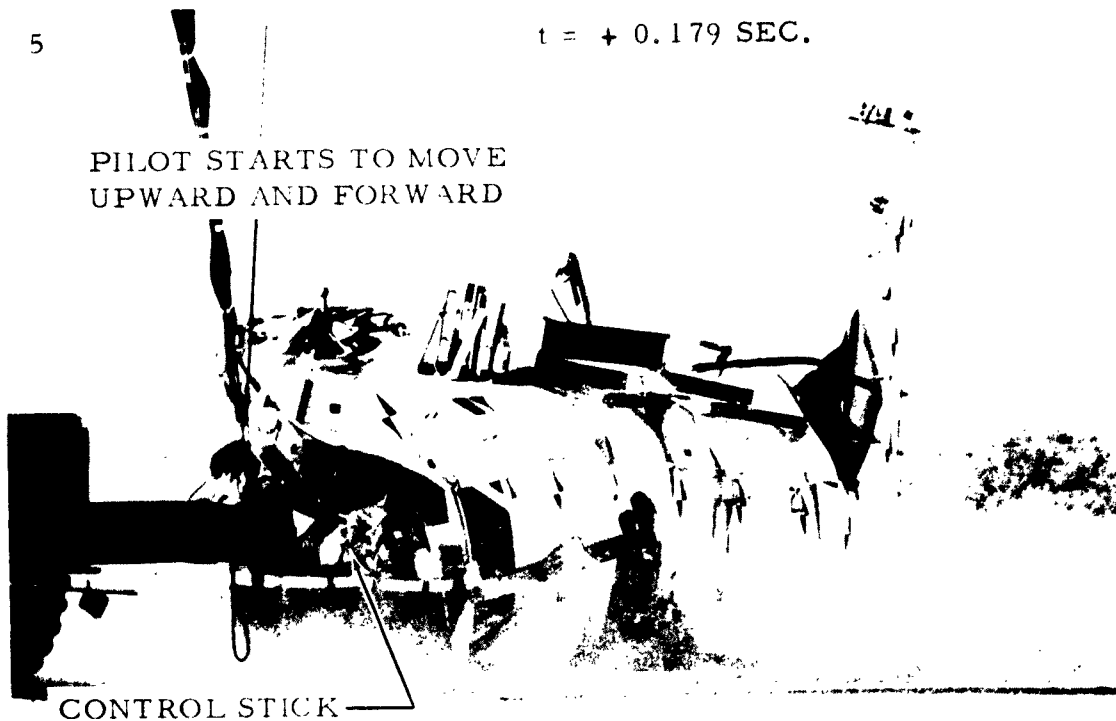


Figure 40-5. Sequence Photograph, H-25 Drop Test

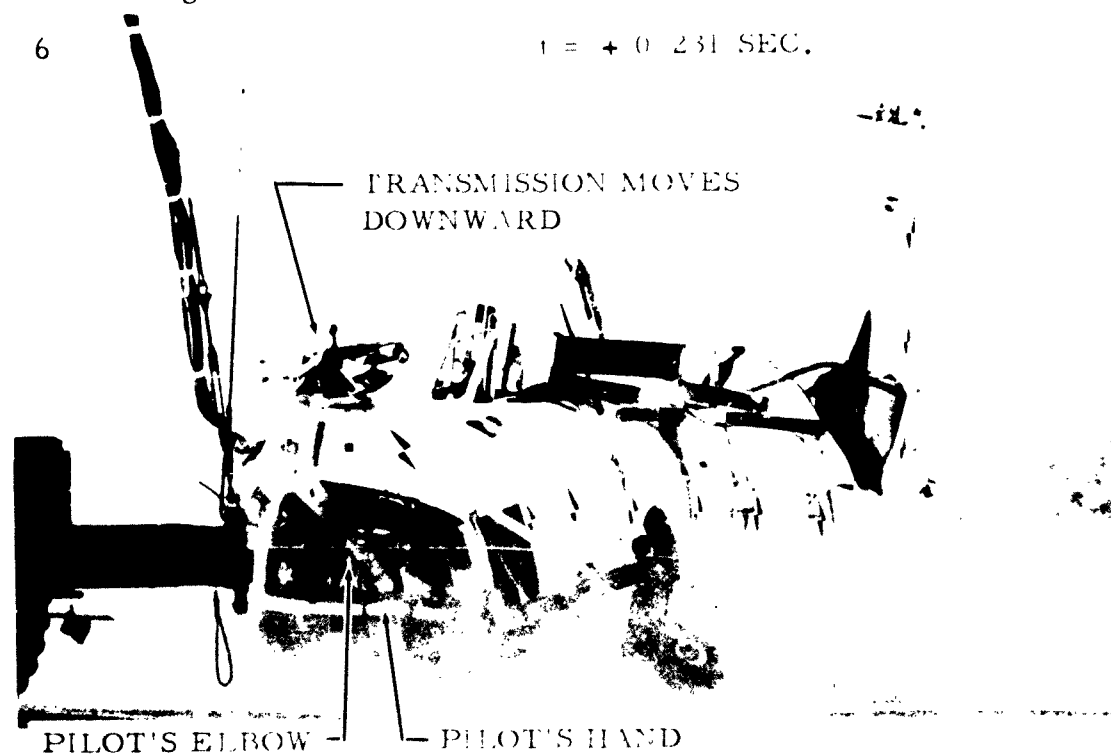


Figure 40-6. Sequence Photograph, H-25 Drop Test

7

t = + 0.439 SEC.

TRANSMISSION LIFTING
TO NEAR NORMAL POSITION

RANGE EXTENDER TANK
MOVES INTO CONTROL PEDALS



PILOT'S HAND MOVING FORWARD
INTO INSTRUMENT COLUMN

Figure 40-7. Sequence Photograph, H-25 Drop Test

8

POST CRASH

RANGE
EXTENDER
TANK



FUEL

PILOT'S HEAD AGAINST STRUCTURE

Figure 40-8. Sequence Photograph, H-25 Drop Test

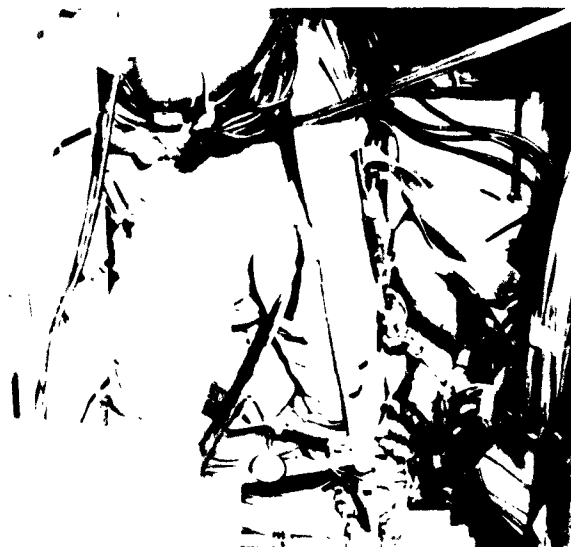


Figure 41. Pilot Dunn: Position Before and After Impact

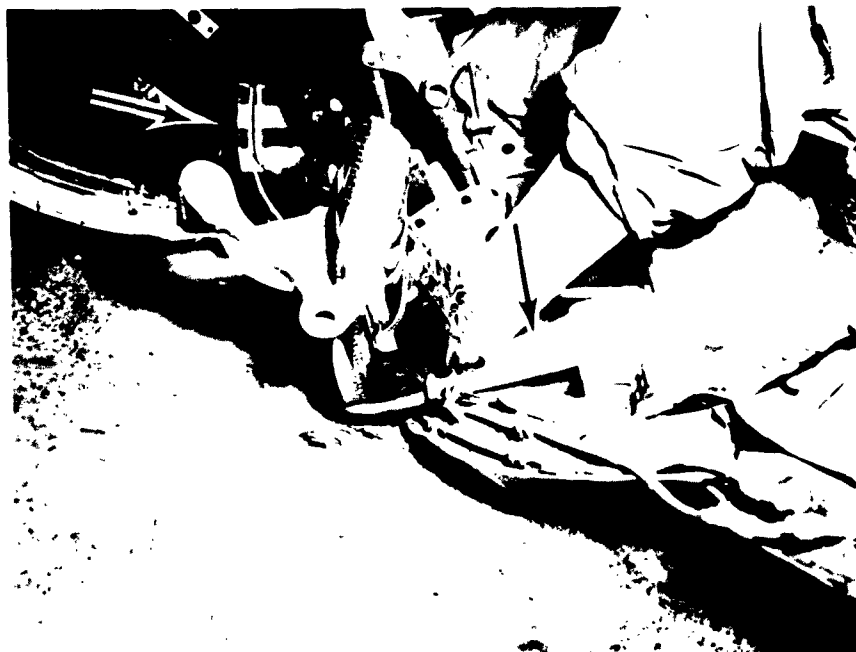


Figure 42. Position of Pilot's Feet Before and After Impact

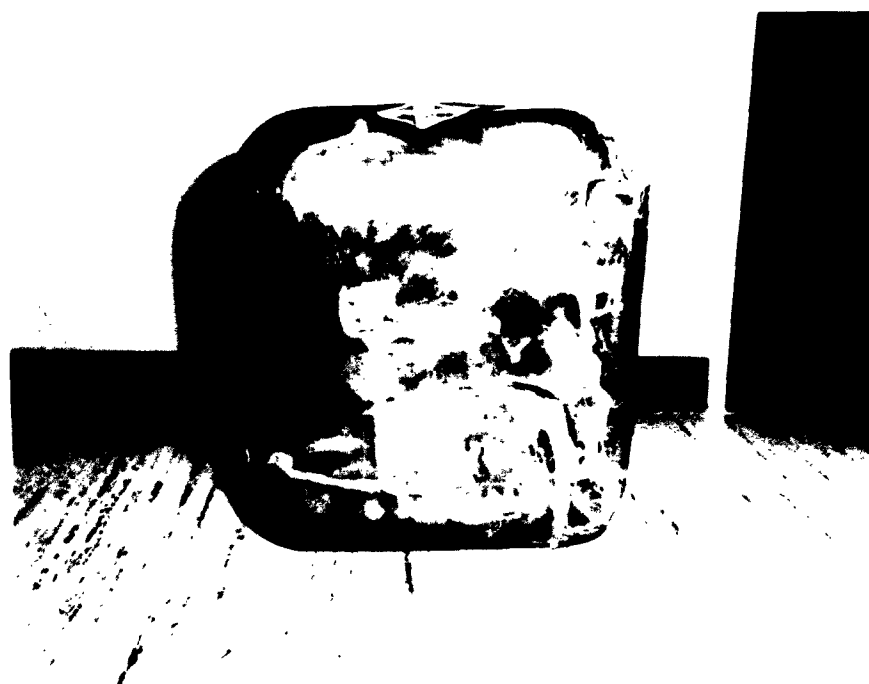
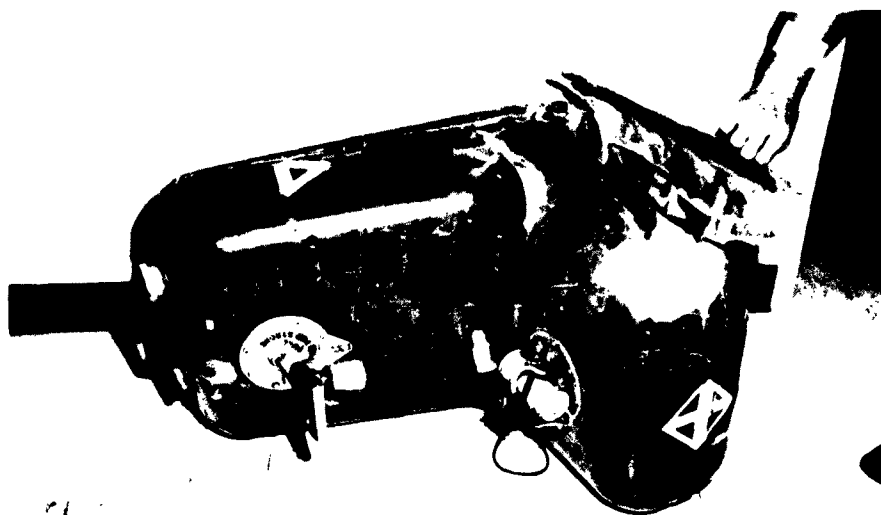


Figure 43. Range Extender Tank Failures

OCCUPANT INJURIES

It is recognized that no direct correlation can be made between "injuries" of the two dummy occupants of the aircraft and the injuries which would have been sustained by an actual pilot and passenger. The following comments are thus presented for their information value only.

PILOT

1. The right hand was driven into the instrument column with sufficient force to bend the hand backward to an angle of less than 90 degrees with the forearm. Index finger and thumb of dummy were damaged. (See Figure 25.)
2. Evidence of considerable force in the ankles existed. (See Figure 42.) The right hand foot was pushed under or around the right hand anti-torque pedal.
3. The head impacted the main fuselage ring, splitting the visor and cracking the helmet (Army APH-5) as shown in Figure 41; however, the helmet remained intact and was not permanently dented. Some damage to the airframe structure did occur in the vicinity of the point of impact (Figure 41), but this damage was apparently due to compression and bending loads in the fuselage frame introduced by the deceleration of mass of the forward transmission system. The fiber-glass fairing over the fuselage frame was destroyed by the impact.

An 80G* longitudinal acceleration in the head was recorded at the moment of contact with the frame. The lateral acceleration record shows the accelerometer to have bottomed at 12G*.

4. A vertical acceleration of 60G in the pelvic region and 51G in the chest region were recorded. An average pelvic acceleration of 30G existed for approximately 40 milliseconds and was coupled with a simultaneous longitudinal pulse of 43G.

PASSENGER

1. The passenger seat failed allowing the dummy to impact the floor in an upright sitting position with a 56G vertical acceleration being recorded in the chest region.

* Airborne recording, not shown elsewhere in this report.



Figure 44. Passenger Dummy Arm Failure

BLANK PAGE

CONCLUSIONS

It is concluded that:

1. A satisfactory and relatively inexpensive method for the simulation of accidents of helicopters has been developed. The method permits the use of ground-mounted instrumentation.

The approximate limitations are:

Maximum gross weight	6,000 lbs.
Maximum horizontal velocity	30 m.p.h.
Maximum vertical velocity	30 m.p.h.

The method is extendable to accidents involving hot engines for the study of post crash fires.

2. Reliable acceleration data for both the airframe and dummy occupants have been obtained in a typical crash of an H-25A Piasecki helicopter.
3. On the basis of this test for an H-25 aircraft accident involving an impact in a 3-point attitude at 30 m. p. h. in both the horizontal and vertical directions, peak accelerations may be expected to be of the order of:

Airframe:

Vertical acceleration at the floor	100G
Horizontal acceleration at the floor	50G

For a normally seated pilot or copilot:

Vertical pelvic acceleration	60G
Longitudinal pelvic acceleration	25-40G

For a normally seated passenger:

Vertical pelvic acceleration	50G*
Longitudinal pelvic acceleration	35G*

* Occur upon final impact with the floor following seat failure.

4. Pilot, copilot, and troop seats, designed to present military standards, can be expected to fail in this aircraft in accidents of this severity.
5. A significant difference has been observed to exist between the acceleration pulses recorded in the occupiable area of the H-25 aircraft in this test and those recorded in the cabin area of larger transport aircraft which were subjected to crash tests by NACA. * With reference to Figure 39, it is evident that short duration high G accelerations existed for the H-25, while longer duration lower level accelerations occurred in the transport. The accident conditions were not entirely comparable for the two aircraft; however, this difference in the acceleration pulses may be expected to occur even under identical conditions. The small deceleration distances applicable to the smaller aircraft, and the low energy absorption capacity of the lighter sheet metal structure, will both tend to yield higher (and shorter duration) accelerations for the small helicopter. A high incidence of deceleration injuries might thus be expected with these aircraft as compared to the transport.
6. The feasibility of airborne recording has been established. Except for a system disturbance of undetermined origin, satisfactory airborne recording would probably have been accomplished in this test, even though equipment which is not normally recommended for this purpose was used. Magnetic tape recorders, capable of sustaining high G loads during operation, are being considered for possible use in future tests.
7. The installation of Mark XII range extender tanks in service aircraft should be made in only those regions of the airframe which will allow maximum isolation of the tank from the structure in event of accident. Failures in the bottom of the tank may be expected when used with normal seat cushions. Contoured cushions are recommended. The extensive failure of the seam between the two halves of the tank suggests that further study and development of these devices is needed.

* G. Merritt Preston and Gerard J. Pesman, "Accelerations in Transport-Airplane Crashes", National Advisory Committee for Aeronautics (NACA TN 4158).

APPENDIX A
VARIOUS METHODS OF SIMULATING CRASH CONDITIONS

BLANK PAGE

VARIOUS METHODS OF SIMULATING CRASH CONDITION

The following methods of duplicating the test conditions outlined on page 7 were considered in order to insure that the most reliable of the methods, with due consideration of cost and simplicity of operation, would be selected:

1. Vertical drop of the helicopter onto an inclined plane;
2. Swinging the helicopter as a pendulum onto level ground;
3. Releasing the vehicle down an inclined monorail; and
4. Dropping the helicopter onto level ground using a moving crane.

The methods investigated are described in the following paragraphs listing the advantages and disadvantages of each:

1. Vertical Drop onto Inclined Plane

- a. Description

In this method, the specimen would be dropped onto a prepared surface inclined at an angle β with the horizontal.

The specified forward (horizontal) and vertical velocities determine the slope of the inclined plane.

$$\alpha = \tan^{-1} \frac{29 \text{ miles per hour}}{35 \text{ miles per hour}} \quad \begin{array}{l} \text{(vertical velocity)} \\ \text{(horizontal velocity)} \end{array}$$

$$\alpha = 40^\circ \quad \text{with vertical}$$

$$\beta = 50^\circ \quad \text{with horizontal}$$

The acceleration of gravity during free fall would impart the specified resultant velocity of 45 miles per hour (66 feet per second) to the helicopter.

APPENDIX A

The drop height was determined from the equation:

$$h = \frac{v^2}{2g}$$
$$h = \frac{66^2}{2(32.2)} = 67.7 \text{ ft.}$$

A crane would be required to lift the helicopter to the required drop height.

A sketch of the proposed method is presented as Figure A-1.

b. Advantages

(1) Simple mechanics of method increases reliability.

c. Disadvantages

(1) Cost of surface preparation at the required angle.

(2) Arrestment of vehicle after crash produces a second impact.

(3) Difficulties of working on such a grade during test set-up and test periods.

(4) Undesirable angle for ground photographic coverage.

(5) Inability to change condition.

(6) Complicated hoisting arrangement for lifting vehicle at required angle.

2. Pendulum Method

a. Description

The specimen would be hoisted to the drop height (67.7 feet as in Method 1) necessary to produce the 45 miles per hour resultant velocity, using a crane. A parallelogram type cable system, to provide stability, would be connected between the specimen and a tower. The pendulum pivot point would be located near the top of the tower at a point higher than the release point in order to improve release stability. At release the specimen would swing as a pendulum contacting level

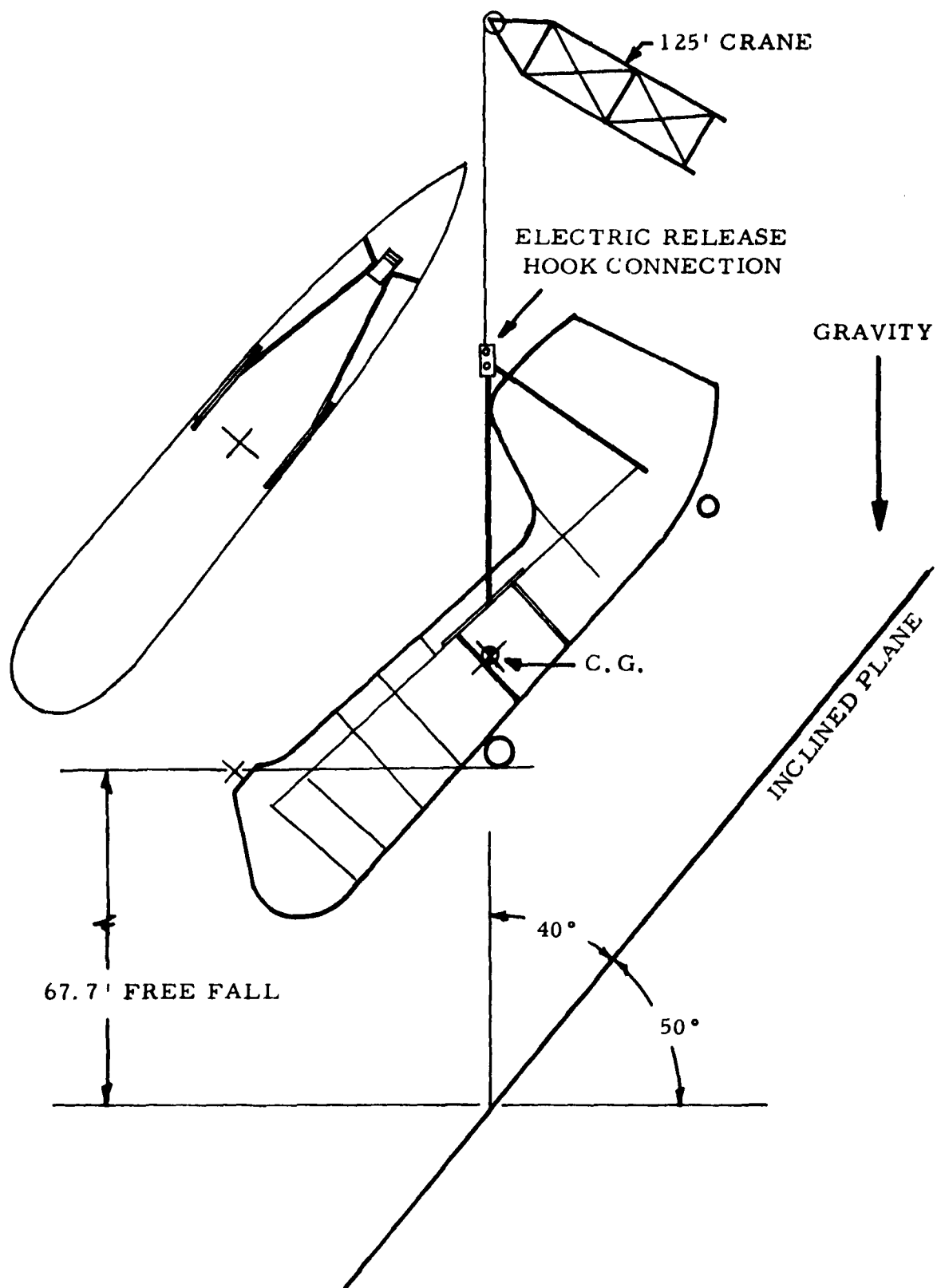


Figure A-1. Proposed Test Method of Dropping Specimen onto 50° Inclined Plane

APPENDIX A

ground at the required 40° impact angle and with a 45 miles per hour resultant velocity. The geometry of the pivot point, release point, and ground would be such as to satisfy the specified crash condition.

A sketch of the proposed method is presented as Figure A-2.

b. Advantages

- (1) Flexibility of set-up in varying test condition by changing geometry of pivot and release points with ground.
- (2) The ability to impact onto a target on level ground under controlled conditions.

c. Disadvantages

- (1) Cost of set-up
- (2) Attachment of guide cables to specimen

3. Inclined Monorail Method

a. Description

The helicopter would be placed on an overhead inclined monorail at a location above the impact point necessary to produce the required vertical velocity by the acceleration of gravity.

The monorail would be inclined at an angle of 40° with the horizontal to satisfy the specified flight path velocity. At release, the specimen would move down the incline leaving the rail at the instant of impact. This would allow the helicopter to crash as a free body.

A winch located at the upper end of the monorail would be used to raise or lower the specimen to the release position.

A sketch of the proposed method is presented as Figure A-3.

b. Advantages

- (1) The ability to crash onto a target on level ground under controlled conditions.

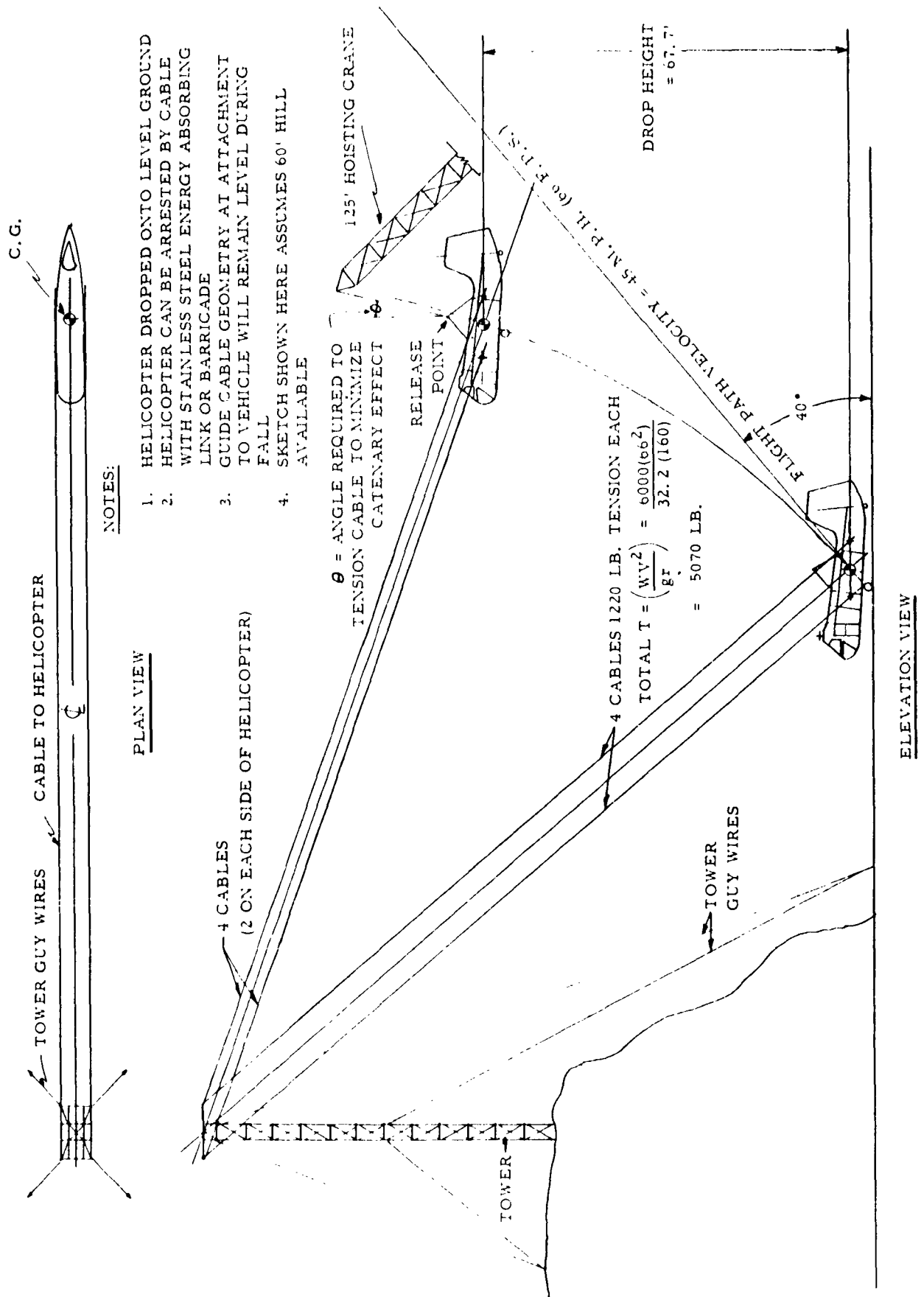


Figure A-2. Proposed Layout for Swinging Helicopter as a Pendulum.

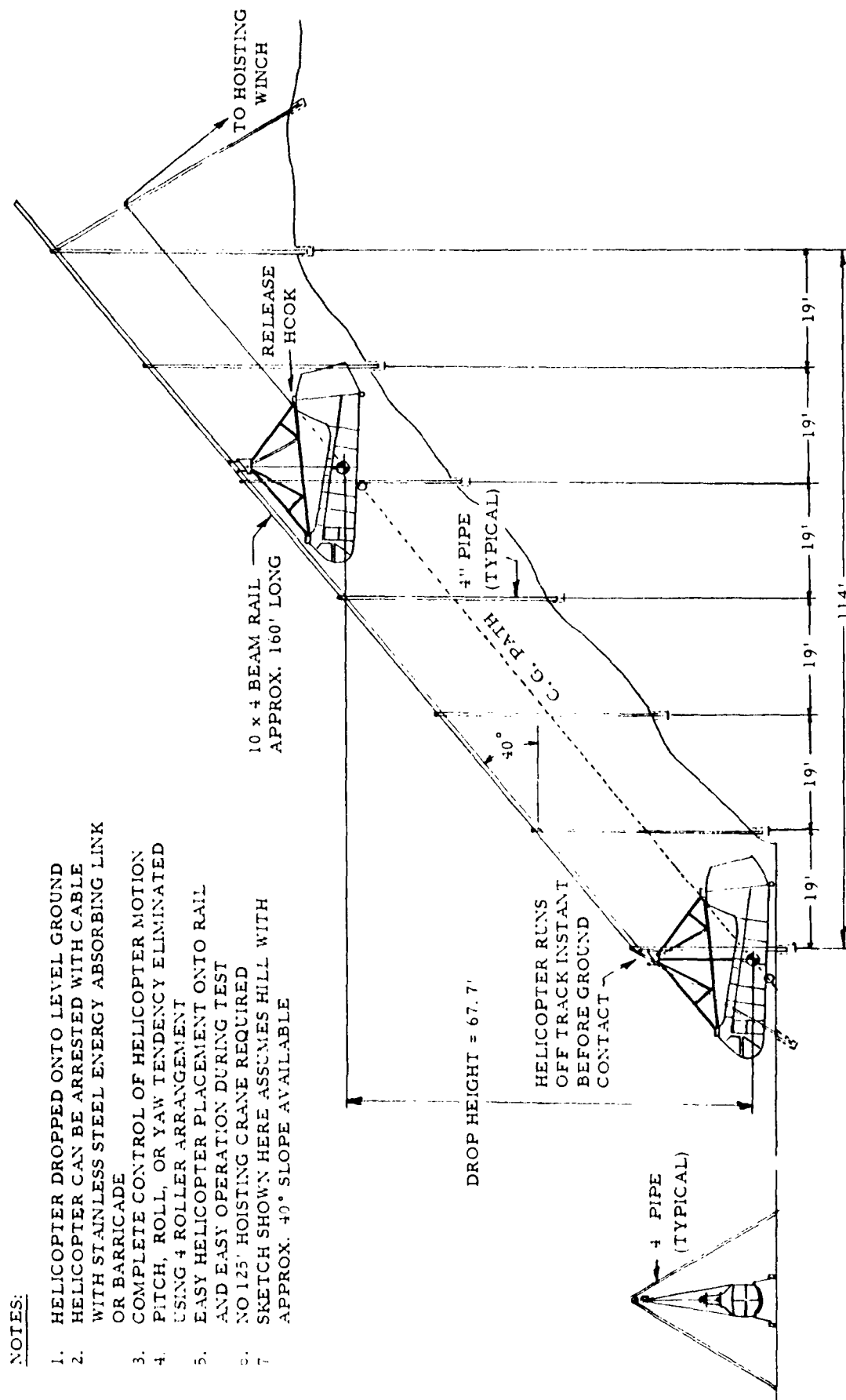


Figure A-3. Proposed Layout for Test Using Monorail System.

(2) No lift crane required.

c. Disadvantages

(1) Cost of set-up.

(2) Inability to change test conditions.

4. Moving Crane Method

a. Description

The helicopter would be suspended from the boom of a hoisting crane vehicle at a 28-foot distance above the ground in order to produce the specified 29 miles per hour vertical velocity by means of free fall. The crane vehicle would accelerate to the required 35 miles per hour forward velocity and release the helicopter allowing it to drop onto level ground at the specified flight path velocity.

A sketch of the proposed method is presented as Figure A-4.

b. Advantages

(1) Relatively low cost of system.

(2) Simplicity of set-up.

c. Disadvantages

(1) Requires ground instrumentation equipment to be mounted on a moving vehicle.

(2) Smooth crane running surface required.

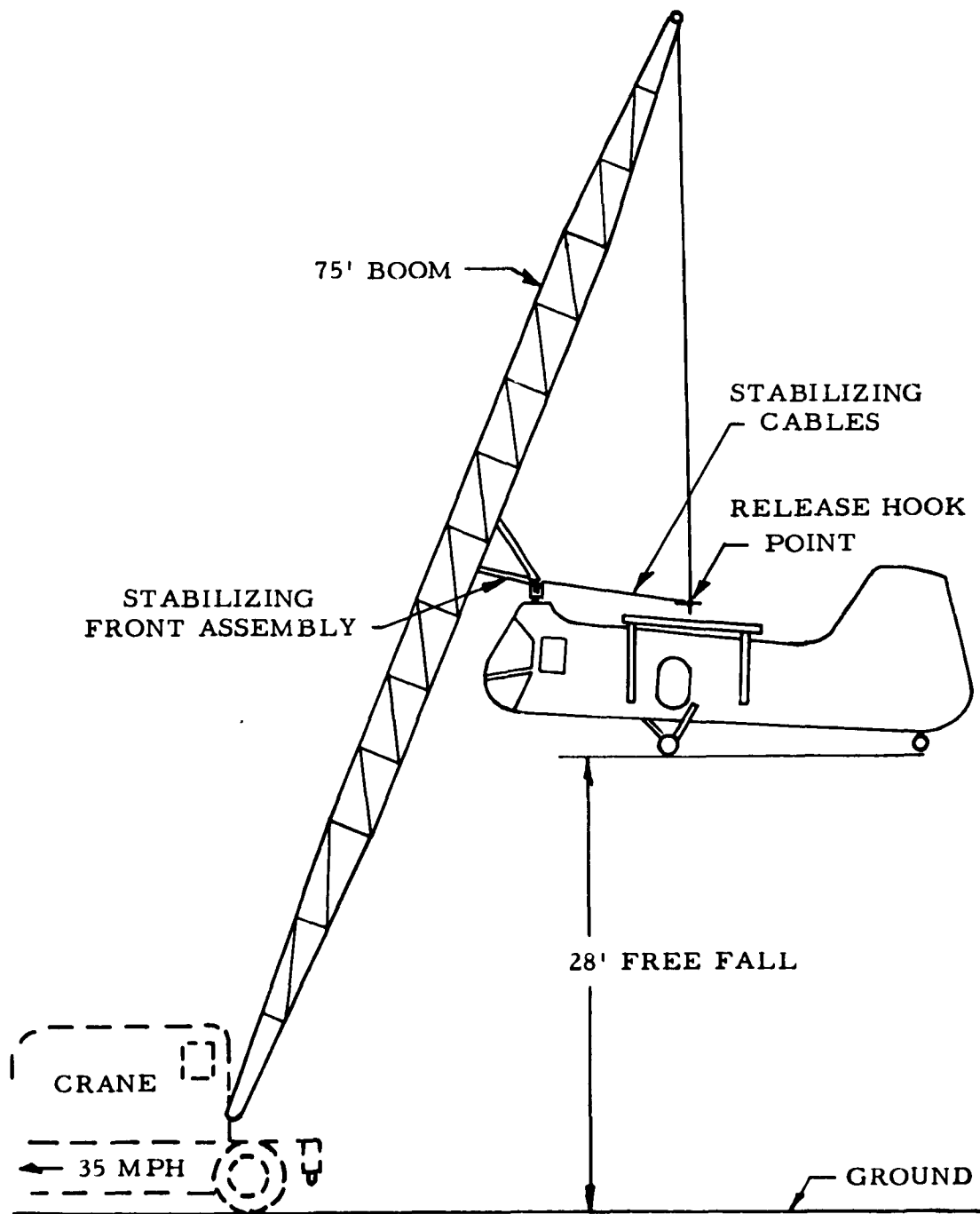


Figure A-4. Proposed Test Method Using Moving Crane to Drop Helicopter on Target While Moving at 35 M. P. H.

APPENDIX B

DEVELOPMENT-TESTING

OF

ENERGY ABSORPTION SYSTEM

FOR

THE SHOCK-MOUNTING OF AIRBORNE ELECTRONIC EQUIPMENT

BLANK PAGE

DESIGN, TESTING, INSTALLATION, AND OPERATION OF SHOCK
DEVICE FOR AIRBORNE ELECTRONIC EQUIPMENT

The second objective of the H-25A helicopter crash test program was to determine the feasibility of an independent airborne oscillographic recording system. The manufacturer of the equipment used in this test would not guarantee its proper operation at accelerations exceeding 15G's. It was necessary to shock-mount this equipment since accelerations anticipated during this test ranged from approximately 100G's on the cockpit and cabin floors to 40G's on the upper fuselage structure.

The equipment requiring this shock-mounting consisted of the following:

	<u>Weight</u>
1 - CEC 5-122 Oscillograph	85 lbs.
1 - CEC 5-053 Timer	4 lbs.
1 - Leland SE-2 Inverter	<u>43 lbs.</u>
Total Weight	132 lbs.

A container was designed to house the equipment. It contained styro-foam packing up to 4 inches thick to protect the equipment from a shock-loading in excess of 25G's in event of a shock absorption device failure.

The container was vented to prevent excessive heating of the enclosed electronic equipment during pre-drop check-out of the system. The container size was 20" wide x 40" long x 16" deep.

Design of Energy Absorption System

General Design

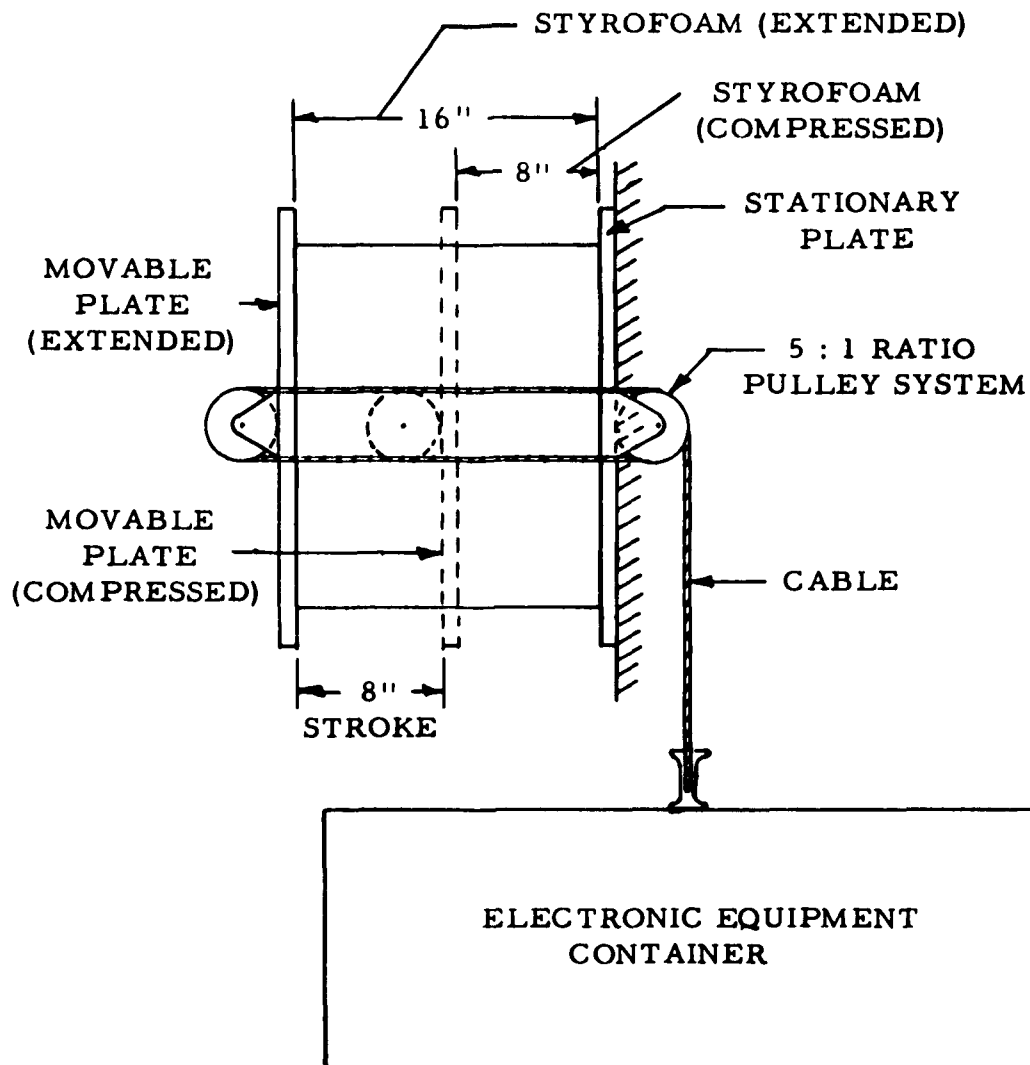
Due to the size of the electronic package container, it was necessary to locate the vertical shock device outside and on the top of the helicopter. Since the structure in this area was not designed for large vertical loads, it was necessary to keep the weight of the system at a minimum.

Dow styrofoam was selected as the energy absorption material because of its light weight (2 lbs. per ft.³) and high efficiency (75-80 percent dynamic).

APPENDIX B

The system would absorb energy by the squeezing of a block of styrofoam between two plates. A 5:1 pulley ratio was used to increase the squeezing load so that the styrofoam block would be shaped approximately as a cube. This increased the stability of the system. The electronic package was attached to the system by means of a cable.

Schematic Design



A photograph showing the energy absorption device and electronic package installation in a test rig is presented as Figure B-1. A photograph of the shock device after having absorbed its design energy is presented as Figure 18.

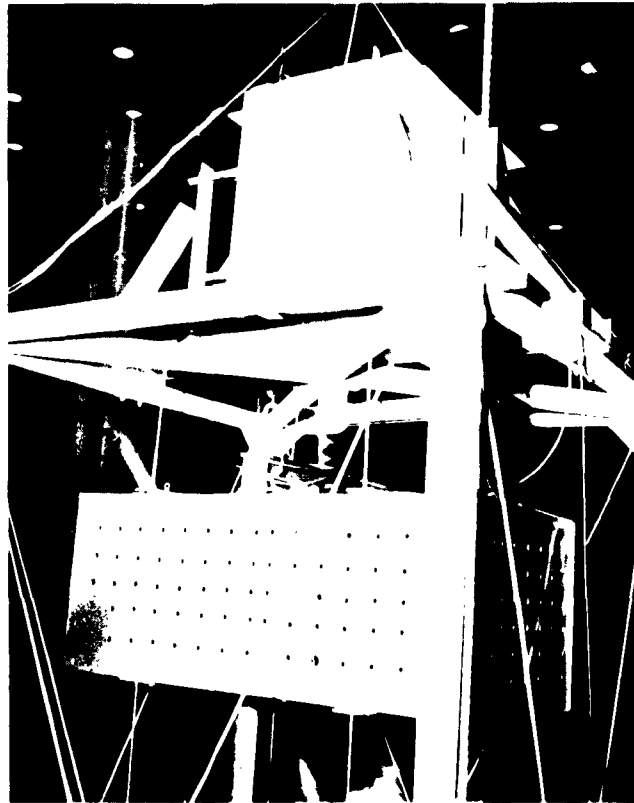


Figure B-1. Oscillograph Shock-Mount Test Set-Up Showing Energy Absorption Device and Electronic Package Before Drop

Design Criteria

Mass to be shock-mounted:

Electronic Equipment	132 lbs.
Container	121 lbs.
Total	<u>253 lbs.</u>

Velocity of Mass (Electronic Package)

Vertical Velocity	= 42.5 ft. per sec. (29 mph)
Forward (Horizontal) Velocity	= 51.3 ft. per sec. (35 mph)
Resultant Velocity	= 66.0 ft. per sec. (45 mph)

APPENDIX B

Energy

$$E = \frac{1}{2} MV^2$$

$$E = \frac{1}{2} \left(\frac{253}{322} \right) (42.5)^2 = 7,090 \text{ ft. - lbs. (85,000 in. - lbs.)}$$

Energy Absorption Material

Dow Styrofoam (2 lbs. per ft.³)

Dynamic Loading at 50% deflection = 32.5 psi

Vertical "G" Loading Desired = 10 "G's"

Load on Electronic Package Support = 10 x 253 = 2,530 lbs.

Load on Styrofoam using 5:1 Pulley Ratio = 5 x 2,530 = 12,650 lbs.

Area Styrofoam required at 50% deflection (Dynamic)

$$\frac{12,650}{32.5} = 390 \text{ sq. in.}$$

Area 19" x 22" used = 420 sq. in.

$$\begin{array}{l} \text{System Stroke Requirement} \\ \text{75\% Efficiency Styrofoam (dynamic)} \end{array} = \frac{85,000}{12,650 (.75)} = 8.3''$$

Styrofoam Block Size = 19" x 22" x 16"

Vertical Movement Package = 8 x 5 = 40"

Efficiency of System (Dynamic) = approximately 75%

Test Program

In order to develop the most optimum energy absorption system and to verify the operation of the actual electronic equipment package, a test program was conducted.

A bird-cage type test-structure was constructed. The shock device and electronic package was installed into this fixture (see photograph, Figure B-2). The bird cage was dropped from a height of 25 feet to subject the package to the

40-feet-per-second terminal velocity anticipated during the helicopter crash. The bird cage was dropped onto styrofoam blocks to subject it to the 40G loading anticipated on the helicopter structure to which the shock device would be mounted. Photographs showing the test set-up prior to dropping, ready for drop, and after dropping, are presented as Figures B-2 through B-4.

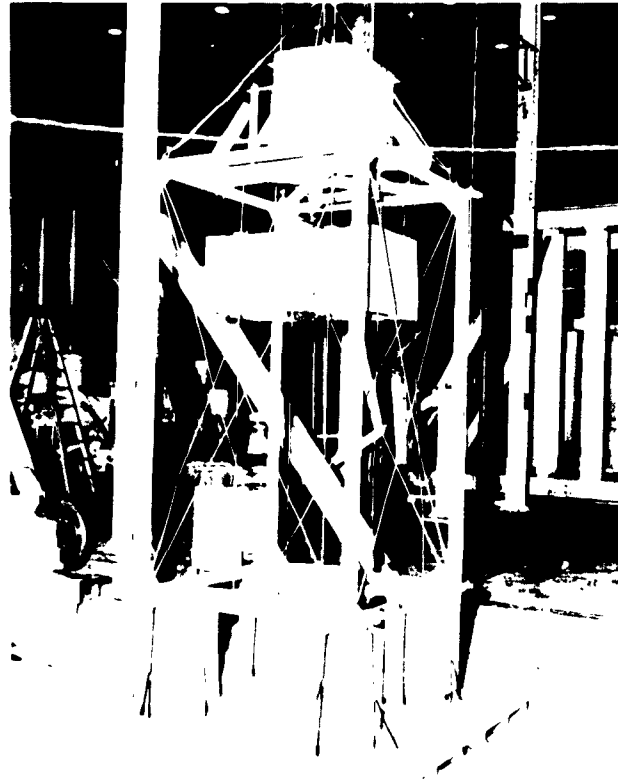


Figure B-2. Set-Up for Test of Oscillograph Shock-Mount

During these tests, the design of the shock device was optimized with the following design established:

Styrofoam size: 19" deep x 22" wide x 16" long

Stroke: 7" at 44% styrofoam deflection

Vertical Movement of Package at 5:1 Ratio Stroke to travel: 34"

Maximum G Loading on Package: 11.5G's

APPENDIX B



Figure B-3. Oscillograph Shock-Mount Test Ready for a Drop

Figure B-4. Oscillograph Shock-Mount Test Post-Drop View



The tests conducted to establish this design used dummy weights to simulate the electronic equipment. With the design accomplished actual electronic equipment was installed to observe its operation under the anticipated shock conditions of the crash. The equipment operated properly during the test with a good oscillograph record obtained.

Installation of Shock Device and Package in the Helicopter

The shock devices were installed in the helicopter. The vertical device imparting 12G's to the electronic package was installed outside and on top of the helicopter (see photograph, Figure 5). The longitudinal device imparting 8G's to the electronic package was installed on the passenger cabin rear shelf above the fuel cell (see photograph, Figure 15). Four vertical guide cables were connected to the helicopter fuselage structure to guide the package and prevent side sway. The fuselage frame at Station 136.8 was reinforced with a simple truss in order to support the vertical shock-device cable load.

Operation of Shock Device System During Crash Test

The shock system functioned properly during the actual crash test protecting the electronic equipment from the crash environment. The airborne oscillograph operated during the entire impact period producing a record of excellent quality; however, discrepancies have been found to exist between the records obtained by the airborne and ground recorders.

A more detailed description of the performance of the airborne recording equipment is given under the section on "Test Results" in the body of this report.

BLANK PAGE

APPENDIX C

DATA REDUCTION AND INTERPRETATION

BLANK PAGE

DATA REDUCTION AND INTERPRETATIONREMOVAL OF THE HIGH FREQUENCY COMPONENTS

In acceleration measurements of complex structures, "ringing", or the introduction of various natural frequencies of the structure into the acceleration records, is a constant problem. Often "high frequency components" of very large magnitude are observed. This occurs because of the inherent relation between displacement, acceleration, and frequency in sinusoidal oscillations. To illustrate:

If a point is moving harmonically with displacement "X", given by the equation:

$$X = A \sin \omega t$$

then the acceleration of the point is:

$$a = -\omega^2 A \sin \omega t = -4\pi^2 f^2 A \sin \omega t$$

Where:

A = The amplitude of the oscillation

ω = Circular frequency in radians per sec.

$$f = \frac{\omega}{2\pi} = \text{frequency in cycles per sec.}$$

Thus, "a" can be very large even though "A" is small for large values of "f". For the oscillograph record shown,* the 260 cps component gives an acceleration amplitude of 100 G for an oscillation with an amplitude of only 0.0145 inch. These high frequency peaks are probably meaningless insofar as inducing possible injury to an occupant of the aircraft, and have been graphically removed from the final acceleration-time plot as shown in the mean acceleration curve of Figure 26.

VALIDATION OF THE RECORDS

The foregoing method of smoothing the data requires some judgment on the part of the analyst, introducing a possible source of error. However, certain steps can be taken to further check the validity of the final results as follows.

The acceleration-time curves obtained in the test can be integrated and compared with the known change in velocity (or displacement) of the point to which the transducer was attached. For example, from the

* See Figure 26.

APPENDIX C

definition of acceleration:

$$\frac{dv}{dt} = a$$

It follows that:

$$v_2 - v_1 = \int_{v_1}^{v_2} dv = \int_{t_1}^{t_2} a \cdot dt$$

This means that the area under the acceleration-time curve must equal the change in velocity.

For the passenger cabin floor vertical acceleration (Figure 26), the vertical velocity at impact, as obtained from measurements of photographs, was 45 feet per second. This agrees satisfactorily with a computed value of 42.5 feet per second. The integrated acceleration-time curve gives the velocity curve shown at the bottom of the graph. No residual velocity error is seen to exist.

This same analysis has been used in the presentation of the records in Figures 27, 28 and 29, for the vertical acceleration of the cockpit floor, the passenger chest area, and the longitudinal acceleration of the cockpit floor. Referring to Figure 27, it will be seen that a velocity error of only 3 feet per second remains at 0.20 second. Thus, excellent agreement between the integrated acceleration-time curve and the expected value of zero residual velocity is evident.

For the passenger chest region, Figure 28, a residual velocity of 7.8 feet per second has been obtained by the integration of the "a-t" curve. In this case, however, this value cannot be considered as an "error" since:

1. The passenger dummy was partially free to move with respect to the airframe, and the chest area of the dummy thus need not necessarily have the same velocity of even a nearby point of the aircraft at corresponding times.
2. The passenger dummy did not remain oriented in a completely vertical position during the impact.* This would reduce an otherwise anticipated velocity decrease in the vertical direction from 45 feet per second to some lesser value. In fact, any longitudinal

* As observed from the high-speed motion pictures covering this area.

acceleration of the aircraft occurring as, or after, the torso of the dummy fell forward (as shown in Figure 24), would show up as a "negative" or downward acceleration on the vertical accelerometer located within the chest cavity. This would leave an "indicated" residual velocity such as observed in Figure 28.

In Figure 29, which shows the original and "smoothed" oscillograph records for the longitudinal acceleration of the cockpit floor, the velocity-time curve has been obtained as outlined in the foregoing procedure. In addition, the v-t curve has been integrated to give the longitudinal displacement of the floor for the first 0.20 second of the impact. Measured displacements, as obtained from high-speed photographs, are also shown at selected times along the curve. Excellent agreement of the displacements obtained by these two methods is evident.

BLANK PAGE

APPENDIX D

ACCELEROMETER DATA SIGN CONVENTION

BLANK PAGE

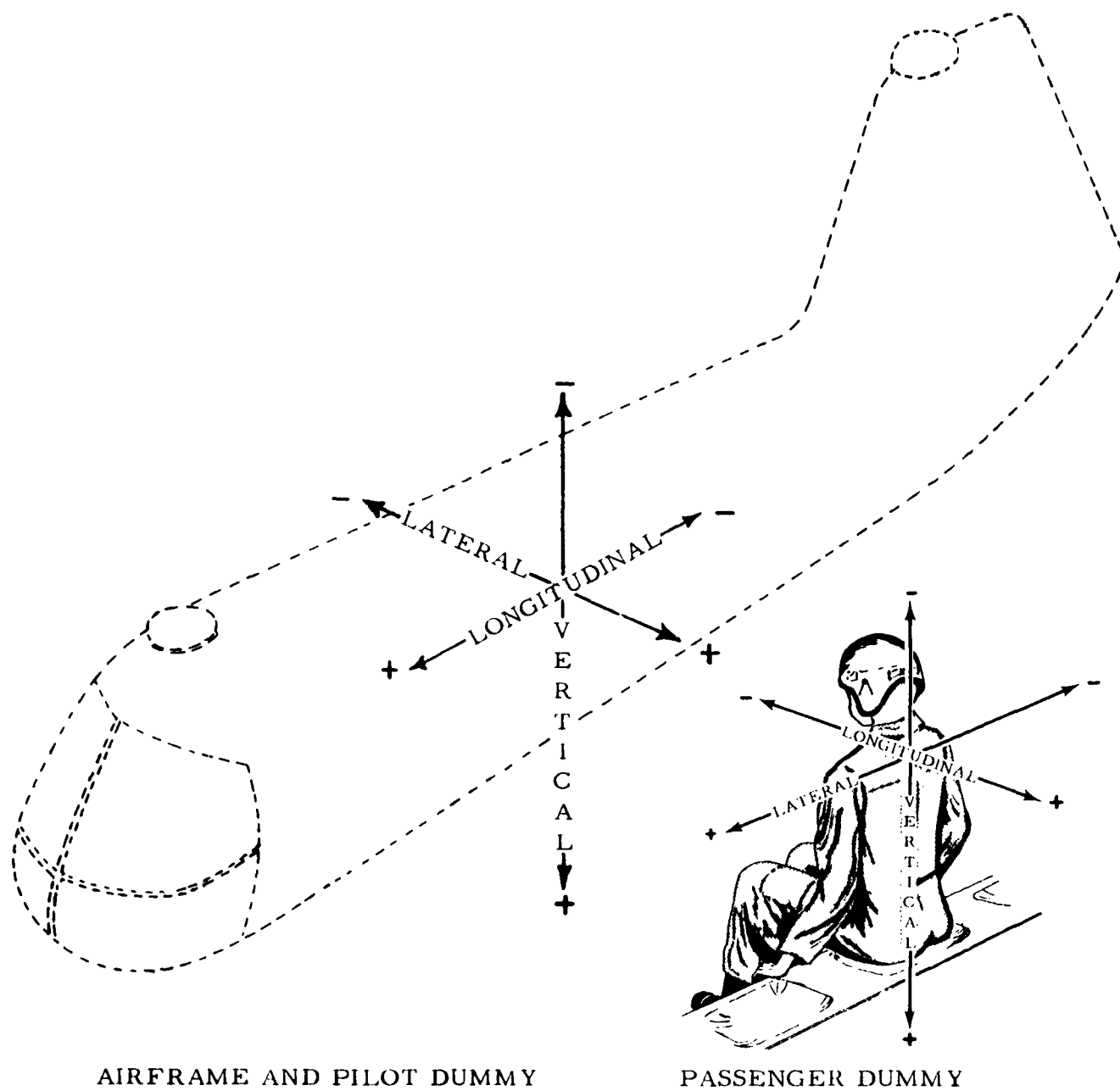


Figure D-1. Accelerometer Data Sign Convention